ACS Catalysis

pubs.acs.org/acscatalysis

Research Article

Structure–Activity Relationships of Hydrothermally Aged Titania-Supported Vanadium–Tungsten Oxide Catalysts for SCR of NO_x Emissions with NH_3

Jun-Kun Lai, Nicholas R. Jaegers, Bar Mosevitzky Lis, Mingyu Guo, Michael E. Ford, Eric Walter, Yong Wang,* Jian Zhi Hu,* and Israel E. Wachs*

Cite This: *ACS Catal.* 2021, 11, 12096–12111

Read Online

ACCESS | Metrics & More | Article Recommendations | Supporting Information

ABSTRACT: Supported V_2O_5–WO_3/TiO_2 materials are employed as selective catalytic reduction (SCR) catalysts for NO_x emission control from power plants. Fresh SCR catalysts usually receive exposure to harsh treatments in the industry to accelerate catalyst activation (calcination in air at 650 °C) and catalyst aging (hydrothermal aging at 650 °C) in a way that represents various points in the catalyst/product lifetime. The present study investigates the catalyst structural and chemical changes occurring during such harsh treatments. Three series of supported V_2O_5–WO_3/TiO_2 catalysts were prepared by incipient-wetness impregnation of aqueous ammonium metavanadate and metatungstate precursors. The catalysts were subsequently dried and calcined at 550 °C in O_2, 650 °C in O_2, and hydrothermal conditions (10% O_2, 8% H_2O, 7% CO_2, and 75% N_2) at 650 °C. The resulting catalysts were physically characterized by numerous techniques (*in situ* Raman; *in situ* IR; *in situ* high-field–high-spinning solid-state ^{51}V MAS NMR; *in situ* electron paramagnetic resonance; X-ray diffraction; Brunauer, Emmett, and Teller surface area; and inductively coupled plasma) and chemically probed with adsorbed ammonia, SCR–TPSR, and the SCR reaction. The surface WO_x sites on the TiO_2 support behave as a textural promoter that stabilizes the TiO_2 (anatase) phase from sintering and transforming to the undesirable crystalline TiO_2 (rutile) phase that can lead to formation of a $Ti_{1-x}V_xO_2$ (rutile) solid solution with reduced V^{4+} cations (~7–15%). The surface VO_x sites are mostly oligomerized as surface $V^{5+}O_x$ sites (~50–85% oligomers) and the extent of oligomerization tends to increase with surface WO_x coverage and calcination temperature. A major difference between the calcined and hydrothermally treated catalysts was the low concentration of surface NH_3^* species on Lewis acid sites for the hydrothermally treated catalysts, yet the SCR activity was almost comparable for both catalysts. This finding suggests that surface NH_4^+*, primarily associated with the surface VO_x sites, are able to efficiently perform the SCR reaction. Given that multiple catalyst parameters were simultaneously varying during these treatments, it was difficult to correlate the SCR activity with any single catalyst parameter. A correlation, however, was found between the SCR TOF/activity and the sum of the surface NH_3^* and NH_4^+* species, which is dominated by the surface NH_4^+* species.

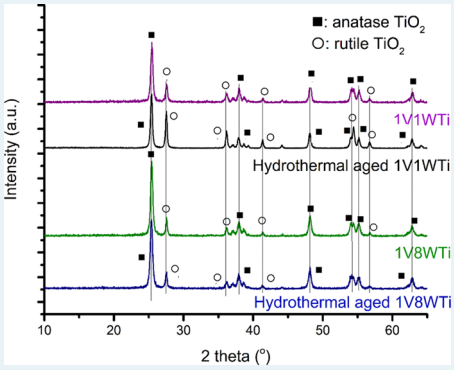

KEYWORDS: *SCR, NO, NH_3, catalyst, V_2O_5, WO_3, TiO_2, promotion, stabilization*

1. INTRODUCTION

The selective catalytic reduction (SCR) of NO_x (NO and NO_2) with NH_3 to harmless N_2 and H_2O products is given by the overall reactions

$$4NO + 4NH_3 + O_2 \rightarrow 4N_2 + 6H_2O \quad (1)$$

$$2NO_2 + 4NH_3 + O_2 \rightarrow 3N_2 + 6H_2O \quad (2)$$

The SCR technology finds industrial application to control NO_x emissions from power plants, industrial boilers, diesel engines (trucks, locomotives, and watercrafts), gas turbines, and gasoline engines (light duty automobiles). The catalysts widely employed in power plants and industrial boilers consist of supported V_2O_5/TiO_2 promoted with other metal oxide materials such as MoO_3 or WO_3. The supported V_2O_5–WO_3/TiO_2 catalysts possess high SCR activity, thermal stability, and resistance to sulfur oxide poisoning.[1−3] The TiO_2 (anatase) support is considered the best performing support for SCR catalysts because (i) both vanadium and tungsten oxides can be uniformly dispersed on the TiO_2 support below monolayer surface coverage, (ii) titania promotes the catalytic activity of the surface vanadium oxide sites, and (iii) titania is not

Received: May 11, 2021
Published: September 15, 2021

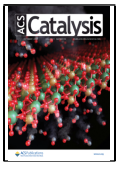

https://doi.org/10.1021/acscatal.1c02130
ACS Catal. 2021, 11, 12096–12111

corroded by the acidic SO_2/SO_3 and NO_x components present in the flue gas.[1,2,4] The vanadium oxide component acts as the catalytic active site that undergoes the redox reaction cycle.[5−7] For such applications, the loading of vanadium oxide is maintained at ∼1−2% V_2O_5 in order to minimize the undesired oxidation of SO_2 to SO_3 and its further conversion to sulfuric acid (H_2SO_4) in the presence of moisture in flue gases.[5,6,8] The tungsten oxide component itself exhibits very low SCR activity in the absence of vanadium oxide, especially at modest reaction temperatures, but acts as a promoter that increases the SCR reaction rate of supported V_2O_5−WO_3/TiO_2 catalysts.[9]

Previous studies with supported V_2O_5/TiO_2 and V_2O_5−WO_3/TiO_2 catalysts calcined at 550 °C demonstrated that at low surface coverage (<0.2 monolayer), the surface VO_x sites mainly present as isolated sites.[6,10] As the coverage of vanadium oxide increases, the surface VO_x sites tend to oligomerize.[6,10] These changes were accompanied by an increased population of surface NH_4^+* species and enhanced SCR activity. Addition of tungsten oxide to the supported V_2O_5/TiO_2 catalysts further increased (i) the extent of surface VO_x oligomerization, (ii) the number of surface NH_4^+* species, and (iii) the SCR activity. The corresponding population of surface NH_3^* species, however, decreased since the majority of surface NH_3^* species were associated with the TiO_2 support and the exposed titania sites decreased as the concentration of surface VO_x and WO_x sites increased. These detailed molecular level studies demonstrated for the first time that surface WO_x sites, which are inactive for SCR, promote the SCR reaction by forming the more active oligomeric surface VO_x sites *via* a geometric effect and not an electronic effect.[7]

High-temperature treatments of ∼500−700 °C are typically applied to fresh catalysts in the industry to accelerate catalyst activation (*e.g.*, calcination at 650 °C) and establish a reproducible testing condition (referred to as "degreening") or to accelerate catalyst aging in a way that represents various points in the catalyst/product lifetime (*e.g.*, hydrothermal aging at 650°).[11−14] Studies with fresh, supported V_2O_5−WO_3/TiO_2 SCR catalysts calcined from 350 to 550 °C have been extensively reported,[6] but fewer studies exist that explore the effect of hydrothermal treatments on the catalyst structures and SCR activity.[15−26] The most detailed study to date about the aging of supported V_2O_5−TiO_2 catalysts under high-temperature calcination and hydrothermal treatments was recently reported by Marberger *et al.*[15,16,27] It was observed that SCR activity initially increases in the 500−600 °C range owing to an increase in the formation of the more active oligomerized surface VO_x sites brought about by the increase in surface VO_x density associated with the loss in surface area of the TiO_2 support. At the higher temperature treatment of 650 °C, the SCR activity decreases, but the origin of the decrease was not fully understood. Activation at 500 °C also resulted in removal of surface sulfate species that were present in this catalyst and an increase in the number of surface NH_3^* species. A more detailed understanding of the changes that take place during the activation and aging of the V_2O_5−WO_3/TiO_2 SCR catalyst is warranted to better elucidate the structural changes of the catalytic active sites and their effects on the SCR reaction.

The current research explores the influence of hydrothermal treatments on the TiO_2 support (surface area, crystalline bulk phases, and surface region), surface VO_x sites [molecular structure and acidity (surface NH_3^* on Lewis acid sites and surface NH_4^+* on Brønsted acid sites)], V^{4+} sites in $Ti_{1-x}V_xO_2$ solid solution,[28] surface WO_x sites (molecular structure and acidity), and the SCR performance. The investigation employs a wide arsenal of characterization techniques [inductively coupled plasma (ICP) analysis of V; Brunauer, Emmett, and Teller (BET); X-ray diffraction (XRD); *in situ* Raman; *in situ* high-sensitivity−low-energy ion scattering (HS-LEIS); *in situ* high-field ^{51}V MAS NMR; *in situ* electron paramagnetic resonance (EPR); and *in situ* IR studies]. The combination of detailed characterization and SCR activity studies establishes unique insights into the structure−activity relationships for this catalytic system.

The findings from the current studies reveal, for the first time, that one of the critical roles of surface WO_x sites on the TiO_2 support is to stabilize supported 1% V_2O_5−*x*% WO_3/TiO_2 catalysts by retarding formation of a poorly active thin surface $Ti_{1-x}V_xO_2$ (rutile) mixed oxide layer under harsh environmental conditions. Secondary well-known important roles of surface WO_x are to stabilize the surface area of the TiO_2 support and retard the bulk transformation of TiO_2 (anatase) to TiO_2 (rutile). For all these negative effects, monolayer quantities of surface WO_x sites are found to be most effective in minimizing these structural changes. The surface VO_x sites are primarily present as oligomeric species due to the high metal oxide surface density after calcination and hydrothermal treatment at 650 °C and minimal volatilization of VO_x. Only a small fraction of $V^{4+}O_x$ dissolves into the TiO_2 (rutile) lattice forming a solid solution after the high-temperature treatments. Surprisingly, the hydrothermally treated catalysts only possess a small amount of surface NH_3^* species on Lewis acid sites and primarily contain surface NH_4^+* species on Brønsted acid sites. Generally, the catalysts lose activity when calcined at 650 °C in O_2 (representative of a freshly activated catalyst) and hydrothermally aged (HTA) at 650 °C (representative of an aged working catalyst), but the activity difference between the activated and aged catalysts is not as significant as previously thought.

2. EXPERIMENTAL SECTION

2.1. Catalyst Preparation. The V_2O_5−WO_3/TiO_2 and WO_3/TiO_2 catalysts were synthesized by incipient-wetness impregnation of aqueous ammonium metavanadate and ammonium metatungstate solutions onto a crystalline TiO_2 support (Evonik, P-25, ∼55 m^2/g, ∼80% anatase). Appropriate volumes of aqueous solutions of ammonium metatungstate (0.06 M) or ammonium metavanadate (0.35 M) were impregnated into the TiO_2 support. After thoroughly mixing for 30 min, the catalysts were dried overnight under ambient conditions with one of the precursors. The impregnation was repeated with the second precursor, and the catalysts were again dried overnight under ambient conditions. Unless otherwise indicated, the first impregnation involved the use of ammonium metatungstate. The catalysts were further dried in flowing dry air at 120 °C for 2 h and finally calcined in flowing dry air at 550/650 °C for 4 h. HTA catalysts were further treated in flowing 10% O_2, 8% H_2O, 7% CO_2, and 75% N_2 at 650 °C for 50 h.

2.2. BET Surface Areas. The BET surface areas of both fresh and HTA catalysts were measured by a three-point flow BET method with an Altamira Instruments system (AMI 200) equipped with a TCD detector. Prior to BET surface area measurement, the catalysts were heated at ∼150 °C for 1 h to

https://doi.org/10.1021/acscatal.1c02130
ACS Catal. 2021, 11, 12096−12111

remove residual adsorbed moisture. BET surface area measurements used nitrogen gas as the adsorbate at liquid nitrogen temperature. The N_2 adsorption/desorption amounts were measured at three different partial pressures (P/P_0 = 0.14, 0.22, and 0.30) for the calculation of surface area.

2.3. XRD Analysis. The XRD patterns were measured with a Rigaku MiniFlex II diffractometer using Cu Kα radiation (1.5418 Å). Full scans of 10−70° (2θ) were measured with a scan rate of 1 °/min. The major peaks at 20−60° (2θ) were measured with a scan rate of 0.1 °/min. The extent of the anatase to rutile phase transition in titania was determined by Rietveld refinement.

2.4. *In Situ* Raman Spectroscopy. The static and time-resolved Raman measurements of the molecular structures of the catalysts were determined with visible (532 nm) laser excitation on a single-stage HORIBA Jobin Yvon Laboratory LabRam HR Raman spectrometer with a confocal microscope (Olympus BX-30) and a notch filter (Kaiser Super Notch). The visible excitation was generated by an Nd-YAG double-diode pumped laser (Coherent Compass 315M-150, an output power of 150 mW with power at the sample of 10 mW). The scattered photons were directed into a single-stage monochromator and focused onto a UV-sensitive liquid N_2-cooled CCD detector (HORIBA Jobin Yvon CCD-3000V) with a spectral resolution of ∼1 cm^{-1} for the given parameters. Powder samples were loaded into a Harrick Scientific cell (HVC-DRP4), which was directly connected to a gas control system consisting of Brooks model 5850E mass flow controllers and a Brooks model 0254 control unit. After catalyst preparation and subsequent calcination or calcination/HTA treatment, Raman spectra of the dehydrated samples were obtained by heating the samples under flowing 10% O_2/Ar for 1 h at 600 °C to dehydrate them. After 1 h at the indicated temperature, the samples were cooled to 110 °C under flowing 10% O_2/Ar, and the Raman spectra were recorded. The temperature of the reaction chamber was controlled by the Harrick ATC Temperature Controller unit.

2.5. *In Situ* HS-LEIS Spectroscopy. The distinction between elements present on the outermost catalyst surface (mostly V and W) and below the outermost surface (Ti) was determined with HS-LEIS spectroscopy. Analysis was conducted with the Qtac^{100} HS-LEIS spectrometer (ION-TOF) equipped with a highly sensitive double toroidal analyzer that provides 3000-fold higher sensitivity than conventional LEIS spectrometers and allows for quantitative dynamic depth profiling. The catalyst samples were prepared for HS-LEIS analysis by compressing the grains within appropriate sample holders (cylindrical dies). Each catalyst sample was initially heated under vacuum in the pretreatment chamber to approximately 80 °C for outgassing. A 10% O_2/Ar mixture was then introduced, resulting in a chamber pressure of 10−12 mbar. The catalyst samples were then dehydrated in the static O_2/Ar environment of the pretreatment chamber at 600 °C for 1 h. After cooling and evacuation of the pretreatment chamber, each catalyst sample was transferred into the UHV chamber containing the HS-LEIS spectrometer for surface analysis. The HS-LEIS spectra were collected over a 1.5 × 1.5 mm raster using a 5 keV Ne^+ ion primary beam with a dose of 2 × 10^{14} Ne^+ cm^{-2} $cycle^{-1}$. Depth profile spectra were obtained by sputtering with 1.0 keV Ar^+ over a 2.0 × 2.0 raster with a total dose of 2 × 10^{16} Ar^+ cm^{-2}. A sputter dose of 1 × 10^{15} Ar^+ cm^{-2} per cycle was used, which removes ∼0.3 nm that corresponds to approximately one monolayer. Prior to calculating the atomic M/Ti (M = V or W) ratios, each elemental spectrum area was corrected using sensitivity factors calculated from the relative integrated intensities of each element compared to a gold standard measured using a 5 keV Ne^+ primary ion beam. The resulting ratios were then normalized using the BET surface area of each sample, thereby correcting for thermally derived surface area loss.

2.6. *In Situ* Solid-State ^{51}V MAS NMR Spectroscopy. All high-field−high-spinning solid-state ^{51}V MAS NMR measurements were conducted with a 14.1 T Bruker 600WB spectrometer utilizing a commercial 2.5 mm pencil-type MAS probe. The corresponding Larmor frequency was 157.778 MHz. Single-pulse NMR experiments were conducted with a 3π/16 pulse width of 1.5 μs, a delay time of 0.2 s, a spectral width of 1 MHz, and an acquisition time of 4.096 ms. Collection of the solid-state ^{51}V MAS NMR spectrum employed at least 500,000 scans. All the NMR spectra were externally referenced to the center band of bulk V_2O_5 at −613.8 ppm relative to $VOCl_3$. All prepared catalyst samples were further dehydrated in flowing dry air at 400 °C before being transferred to an N_2-filled glovebox and loaded into the NMR rotors. The NMR measurements were performed at a set temperature of 25 °C, which corresponds to a spinning-induced temperature elevation to ∼60 °C at the employed spinning rates. Spectral deconvolution was conducted using the DMFIT program, and sample spinning rates of 32−35 kHz were used for all 600 MHz experiments.

2.7. *In Situ* EPR Spectroscopy. All catalyst samples were initially dehydrated in air at 400 °C in flowing dry air before cooling to −148 °C (125 K) for the *in situ* EPR measurements. Continuous wave EPR X-band (9.30 GHz) spectra were collected with a Bruker Elexsys 580 EPR spectrometer. The field was modulated at 100 kHz and a microwave power of 30 dB, with a receiver gain of 80 and four repetitions. The weight percent of vanadium as V^{4+} was calculated using a 0.25 mM aqueous solution of VO_2 dissolved with a small amount of HCl and converted the integrated intensity to equivalent mg of V^{4+} and dividing by the mass of the sample.

2.8. *In Situ* Temperature-Programmed IR Spectroscopy. The time-resolved, TP-IR spectroscopy experiments were performed on a Thermo Nicolet 8700 FTIR spectrometer equipped with a Harrick Praying Mantis Attachment (model DRA-2) for diffuse reflectance spectroscopy and a high-sensitivity mercury−cadmium−telluride (MCT-A) detector. Powder catalyst samples were loaded into the Harrick Scientific cell (HVC-DRP4), and the cell was connected to a gas control system. The Harrick ATC Temperature Controller unit controlled the temperature of the reaction chamber. As the first step in conducting measurements, the samples were dehydrated under flowing 10% O_2/Ar for 1 h at either 450 °C (samples previously calcined at temperatures below 600 °C) or 600 °C (samples previously calcined at 650 °C). After 1 h at the indicated temperature, the samples were cooled to 110 °C under flowing 10% O_2/Ar and IR spectra of the dehydrated samples were recorded. Subsequently at 110 °C, 10% O_2/Ar was replaced by flowing Ar (30 mL/min; 20 min) and then by flowing 2000 ppm NH_3/He (30 mL/min; 30 min). Physisorbed NH_3 was removed by flowing Ar (30 mL/min; 30 min). For SCR reactions with NO, Ar was replaced by flowing 2000 ppm NO/He (30 mL/min), and the catalyst was heated to 450 °C at 5 °C/min. In both cases, IR spectra were recorded at 50 °C intervals.

https://doi.org/10.1021/acscatal.1c02130
ACS Catal. 2021, 11, 12096−12111

2.9. Steady-State SCR Reactivity Studies. The SCR reactivity of the supported V_2O_5–WO_3/TiO_2 catalysts was investigated in a fixed-bed reactor (Altamira AMI-200 temperature-programmed system) equipped with a quartz reactor tube and an online quadrupole mass spectrometer (Dycor Dymaxion DME200MS) for reactant conversion and product analysis. Typically, ~30 mg of catalyst was loaded into a U-type quartz tube and pretreated with 10% O_2/He at 600 °C for 1 h to remove adsorbed organic impurities or moisture and to ensure that the surface VO_x and WO_x species on the TiO_2 support are fully oxidized. The catalyst bed was subsequently flushed with He for 10 min, cooled in He to the reaction temperature, and the SCR reaction mixture was then introduced [35 mL/min of NH_3/He (2000 ppm), 35 mL/min of NO/He (2000 ppm), and 5 mL/min of 5% O_2/He] to obtain a volumetric ratio of NH_3/NO/O_2 of 1:1:3.5. The steady-state SCR reaction was performed for 2 h at several temperatures (200, 250, 275, 300, and 325 °C) to ensure that steady-state reaction conditions were attained. Reaction tests at each temperature were performed in triplicate to confirm the reproducibility of the data. During the SCR reaction, care was taken to avoid heat and mass transfer limitations by employing small particles (~20 nm) and maintaining low NO conversion (~10%).[29] The gases exiting the quartz reactor were analyzed by an online mass spectrometer to determine the rates of reactant conversion (NO, NH_3, and O_2) and reaction product formation (N_2, NO_2, and N_2O). The following mass spectrometer m/z values were employed for the identification of the exiting gases: O_2 (m/z = 32), N_2 (m/z = 28), NH_3 (m/z = 17), NO (m/z = 30), NO_2 (m/z = 46), and N_2O (m/z = 44).

3. RESULTS

3.1. Catalyst Bulk V Content, Surface Area, and Bulk Structure of TiO_2 Support. The V content of the 650 °C calcined and hydrothermally treated catalysts was determined by ICP analysis. The volatilization of VO_x was minor and corresponded to only ~0.02 wt % of V as shown in Table S1. The small loss of VO_x from the hydrothermal treatments did not vary with the tungsten oxide loadings, demonstrating that tungsten oxide content does not influence the volatilization of VO_x from the catalysts under the hydrothermal conditions examined herein. The BET specific surface areas of the catalysts calcined at 550 and 650 °C (in flowing air for 4 h) and the further hydrothermally treated catalysts (650 °C for 50 h in flowing 10% O_2, 8% H_2O, 7% CO_2, and 75% N_2) are listed in Table 1. The bare TiO_2 support possessed a BET surface area of ~55 m^2/g and addition of 1% V_2O_5 and x% WO_3 with calcination at 550 °C slightly decreasing the BET. The 650 °C calcination treatment decreased the BET surface area to ~28–45 m^2/g for the supported V_2O_5–WO_3/TiO_2 catalysts with the loss in BET surface area diminishing with increasing tungsten oxide loading. Hydrothermal aging at 650 °C further decreased the BET surface area of the supported V_2O_5–WO_3/TiO_2 catalysts to 17–37 m^2/g with increasing tungsten oxide loading again diminishing the decrease in BET.

Table 1. BET-Specific Surface Areas for Supported V_2O_5–WO_3/TiO_2 Catalysts after Calcination (650 °C for 4 h in Flowing Air) and Hydrothermal Treatment (650 °C for 50 h in Flowing 10% O_2, 8% H_2O, 7% CO_2, and 75% N_2)

BET surface areas (m^2/g) of supported VWTi catalysts after calcination and hydrothermal aging			
	cal. 4 h (550 °C)	cal. 4 h (650 °C)	hydrothermal 50 h (650 °C)
1V1WTi	51	28	17
1V5WTi	54	40	31
1V8WTi	53	45	37

The XRD diffractograms of the calcined catalysts (650 °C) are given in Figure 1 and show that the TiO_2 (P-25)-containing catalysts are mainly dominated by the TiO_2 (anatase) phase with a smaller amount of rutile phase (~20%) present (see Table S2) and also confirm the absence of the TiO_2 (brookite) phase. The characteristic XRD peaks of the TiO_2 (anatase) phase (major peaks: 2θ at 25.4, 38.0, 48.0, and 54.7°) are all present, and XRD peaks corresponding to crystalline V_2O_5 or WO_3 nanoparticles are not present. Comparison of the XRD diffractograms of the calcined and hydrothermally treated catalysts reveals that the TiO_2 (rutile) phase (major peaks: 2θ at 27.4, 36.1, 41.3, 54.4, and 57.2°) increased from 23 to 42% for supported 1V1WTi and from 19 to 28% for supported 1V8WTi after the hydrothermal treatment. Tungsten oxide, thus, has a significant positive effect on supported V_2O_5/TiO_2 catalysts by stabilizing both the TiO_2 (anatase) bulk phase and its BET during exposure to the harsh hydrothermal environmental conditions.

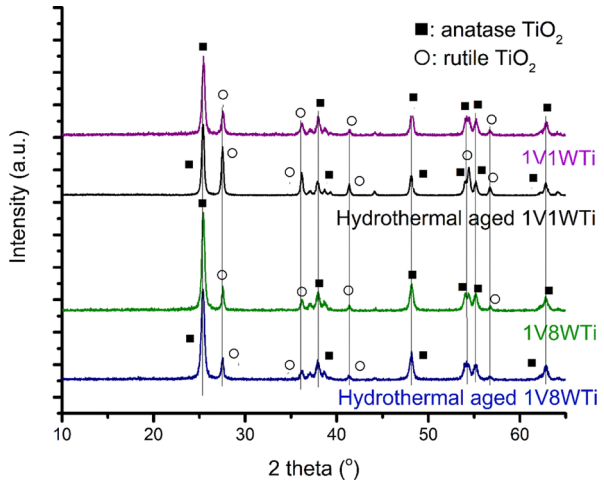

Figure 1. XRD diffractograms of the supported 1V1WTi and 1V8WTi catalysts calcined and HTA at 650 °C.

The Raman spectra for the TiO_2-supported V_2O_5–WO_3 catalysts from the bulk region of the TiO_2 support (200–700 cm^{-1}) are presented in Figure 2 (figures on right). The initial calcined catalysts exhibit only the vibrations of TiO_2 (anatase), reflecting its structural dominance (~80% in the starting TiO_2 support). Although Raman spectroscopy can readily distinguish between the vibrations of bulk TiO_2 (anatase) (797, 632, 510, and 395 cm^{-1}) and bulk TiO_2 (rutile) (610 and 435 cm^{-1}) phases, the Raman scattering for the TiO_2 (anatase) phase is much greater than for the TiO_2 (rutile) phase, making it difficult to detect small fractions of the TiO_2 (rutile) phase in the catalysts.[30−33] The hydrothermally treated catalysts also exhibit the Raman vibrations of the TiO_2 (anatase) phase with exception of the 1V1WTi catalyst that only shows the vibrations of TiO_2 (rutile). The absence of Raman bands from the more efficient scattering of the TiO_2 (anatase) phase indicates that the anatase phase is not present in the outer surface region being sampled by the 532 nm laser and suggests

https://doi.org/10.1021/acscatal.1c02130
ACS Catal. 2021, 11, 12096−12111

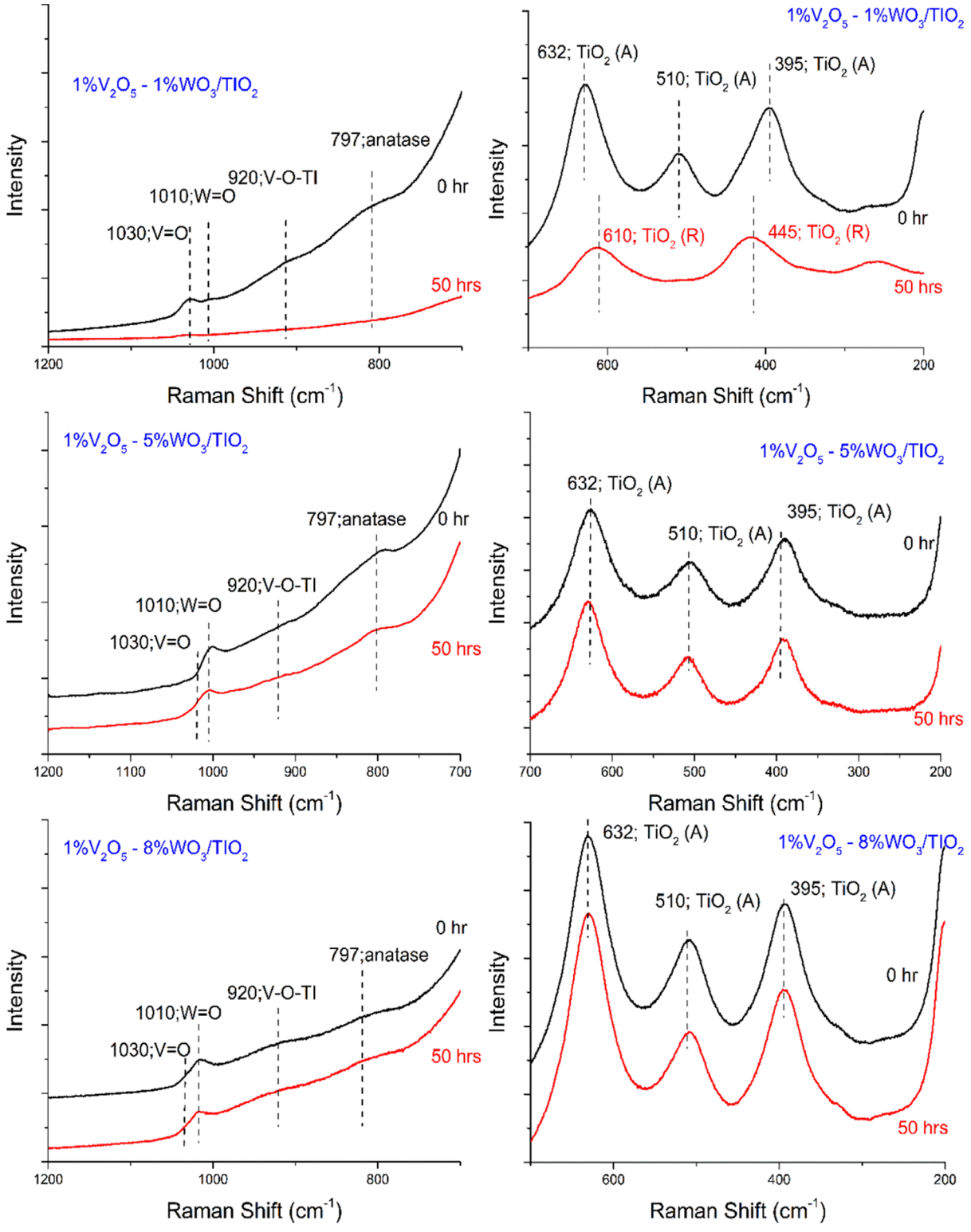

Figure 2. *In situ* Raman spectra of dehydrated, calcined (650 °C for 4 h in flowing air—labeled "0 h" of hydrothermal treatment), and HTA (650 °C for 50 h in flowing 10% O_2, 8% H_2O, 7% CO_2, and 75% N_2) catalysts (supported 1% V_2O_5–x% WO_3/TiO_2 catalysts with x = 1, 5, or 8).

the presence of an outer TiO_2 (rutile) shell layer that encapsulates the inner TiO_2 (anatase) phase (core–shell model).

3.2. *In Situ* Raman Spectroscopy of TiO_2-Supported VO_x and WO_x Phases. The *in situ* Raman spectra of the calcined supported V_2O_5–WO_3/TiO_2 catalysts under dehydrated conditions in the vanadium oxide and tungsten oxide vibrational regions (700–1200 cm^{-1}) are displayed in Figure 2 (figures on the left). The absence of characteristic strong Raman bands from crystalline V_2O_5 (~995 cm^{-1}) and WO_3 (~805 cm^{-1}) indicates that these crystalline nanoparticles are not present in the calcined catalysts. The Raman band at ~1030 cm^{-1} is characteristic of mono-oxo surface $V^{5+}O_x$ sites.[5,6,8] The Raman band at ~1010 cm^{-1} is characteristic of

https://doi.org/10.1021/acscatal.1c02130
ACS Catal. 2021, 11, 12096–12111

mono-oxo surface $W^{6+}O_5$ sites.[5,6,34] The broad band at ~930 cm^{-1} arises from the vibration of the bridging V−O−Ti bond.[5,6,9] The positions of the Raman bands for the surface VO_x and WO_x sites blue-shift (~1027 → 1030 cm^{-1} and 1007 → 1010 cm^{-1}, respectively) with increasing surface vanadia and tungsta coverage from vibrational coupling of adjacent V═O/V═O, W═O/W═O, and possibly V═O/W═O bonds.[10,35−37] Recent cutting-edge high-field, solid-state ^{51}V MAS NMR measurements of supported V_2O_5/TiO_2 catalysts calcined at 550 °C confirm that the surface VO_x sites are predominantly isolated at low surface coverage and progressively oligomerize with increasing surface vanadia coverage on the TiO_2 support.[5,38] The positions of V═O and W═O vibrations, thus, reflect extensive oligomerization of the surface VO_x and WO_x sites on the titania support for the calcined catalysts at 650 °C. The same V═O and W═O vibrations from the catalysts indicate that similar surface VO_x and WO_x sites are present on the calcined catalysts. The supported 1% V_2O_5−8% WO_3/TiO_2 catalyst corresponds to approximately monolayer coverage of surface VO_x and surface WO_x sites on the TiO_2 support as evidenced by the absence of remaining anchoring Ti−OH surface hydroxyls as monitored by *in situ* IR spectroscopy.[39]

The *in situ* Raman spectra of the hydrothermally treated catalysts under dehydrated conditions in the vanadium oxide and tungsten oxide vibrational regions (700−1200 cm^{-1}) also appear in Figure 2 (figures on the left). The supported 1V1WTi catalyst possesses severely diminished Raman bands from the surface VO_x and WO_x sites after the hydrothermal treatment. This may indicate a number of possible scenarios: (i) the weaker Raman scattering from the TiO_2 (rutile) phase relative to that of the TiO_2 (anatase) phase also diminishes the intensity of Raman scattering from the surface metal oxide sites, (ii) surface VO_x is reduced to V^{4+} that is soluble in the TiO_2 (rutile) lattice,[17,38,39,] or (iii) volatilization of VO_x and WO_x into the gas phase during the harsh hydrothermal treatment.[40−43] A small amount of V^{4+} detected by EPR (Table S3) and only trace amounts of vanadium volatilization (Table S1) indicate that the absence of detectable Raman bands from the surface VO_x and WO_x sites is related to the weaker Raman scattering from the outer TiO_2 (rutile) layer of the support in this catalyst. In contrast, the more hydrothermally stable supported 1V5WTi and 1V8WTi catalysts that are dominated by the Raman vibrations of TiO_2 (anatase), with its associated stronger Raman scattering, still exhibit the characteristic Raman bands of the dehydrated surface VO_x and WO_x sites on the TiO_2 support. The same dehydrated surface VO_x and WO_x sites on the TiO_2 support, thus, are present for both the 650 °C calcined and hydrothermally treated supported 1% V_2O_5−5% WO_3/TiO_2 and 1% V_2O_5−8% WO_3/TiO_2 catalysts.

3.3. *In Situ* HS-LEIS Surface Analysis. The HS-LEIS depth profile plots for the supported V_2O_5−WO_3/TiO_2 catalysts are presented in Figure 3a (V/Ti) and 3b (W/Ti). For both the 1V1WTi and 1V8WTi catalysts, the V/Ti ratios monotonically decreased in the outermost surface layer with sputtering depth indicating that V is predominantly present on the outermost surface layer as surface VO_x sites on the TiO_2 supports. The V/Ti ratio at the outermost surface layer slightly increased for the 1V1WTi catalyst upon hydrothermal aging and reflects the increased surface VO_x coverage due to the decrease in the BET surface area (see Table 1). The V/Ti ratio at the outermost surface layer, however, slightly decreased for the more thermally stable 1V8WTi catalyst upon hydrothermal aging. The W/Ti ratio at the outermost surface layer for the 1V8WTi catalyst increased upon hydrothermal aging and reflects the increased surface WO_x coverage due to the decrease in the BET surface area (see Table 1). The W/Ti ratios for the calcined and HTA 1V1WTi catalysts are almost the same. The HS-LEIS findings demonstrate that both vanadia and tungsta are predominantly present as surface VO_x and WO_x sites at the outermost surface layer of the TiO_2 support.

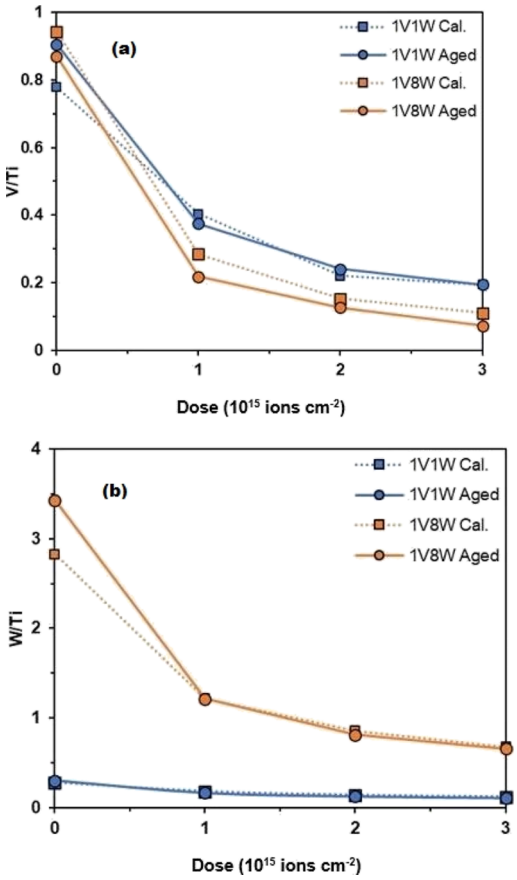

Figure 3. HS-LEIS atomic surface ratios for the dehydrated supported catalysts calcined and HTA at 650 °C: (a) HS-LEIS atomic surface V/Ti ratios for the dehydrated supported 1% V_2O_5−*x*% WO_3/TiO_2 catalysts calcined and HTA at 650 °C; (b) HS-LEIS atomic surface W/Ti ratios for the dehydrated supported *x*% V_2O_5−*y*% WO_3/TiO_2 catalysts calcined and HTA at 650 °C. Depth profile spectra were obtained by sputtering with 1.0 keV Ar^+ [sputter dose of 1 × 10^{15} Ar^+ cm^{-2} corresponds to about one layer (~0.3 nm)].

3.4. *In Situ* Solid-State High-Field−High Spinning ^{51}V MAS NMR. The *in situ* solid-state ^{51}V MAS NMR spectra for the dehydrated titania-supported vanadium oxide catalysts that were HTA and calcined at 650 °C are presented in Figures 4 and S1, respectively. The ^{51}V MAS NMR peak assignments are based on prior experimental studies and density functional theory based theoretical calculations.[5,38] The isolated surface VO_x sites have been assigned to the peaks between −480 and −529 ppm. The dimeric and higher oligomeric surface VO_x sites have been assigned to the peaks at −555 to −630 ppm. The crystalline V_2O_5 nanoparticles or larger 2D surface oligomeric sites give rise to the peak at −613 ppm with higher tungsten oxide loadings. The peaks between −530 and −555 ppm, however, are challenging to assign due to the technical limitations from the prior literature NMR studies.

https://doi.org/10.1021/acscatal.1c02130
ACS Catal. 2021, 11, 12096−12111

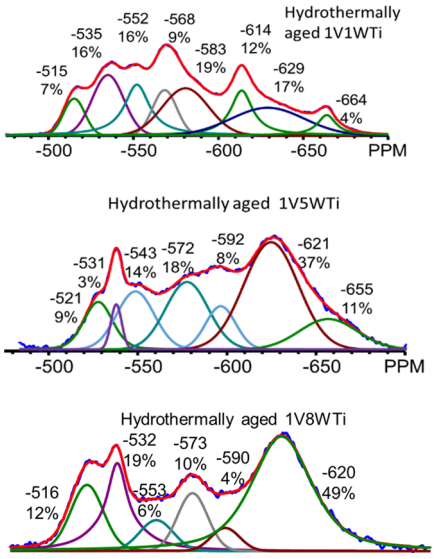

Figure 4. Solid-state ^{51}V MAS NMR spectra of dehydrated supported V_2O_5–$x$$WO_3$/$TiO_2$ catalysts that have been HTA at 650 °C.

The extensive overlap of the resonant peaks from different surface vanadia sites require suitable sets of standard samples to further clarify possible surface VO_x structures on the TiO_2 support. Based on prior computational work and ^{51}V MAS NMR experimental results, the ^{51}V NMR peaks can be assigned as an array of isolated surface VO_x sites on the titania support: distorted VO_4 with a nearby OH or oxygen vacant VO_4 (−480 ppm), distorted VO_4 (−507 ppm), and distorted VO_5 (−533 ppm).

The percentages of oligomeric surface VO_x sites as a function of catalyst composition and treatments [calcined at 550 °C,[5] calcined at 650 °C (Figure S1), and HTA at 650 °C] as determined by solid-state ^{51}V MAS NMR of the dehydrated supported V_2O_5–$x$$WO_3$/$TiO_2$ catalysts are presented in Figure 5. For the 550 °C calcined catalysts, the percent of oligomeric surface VO_x sites increases with surface WO_x coverage.[5]

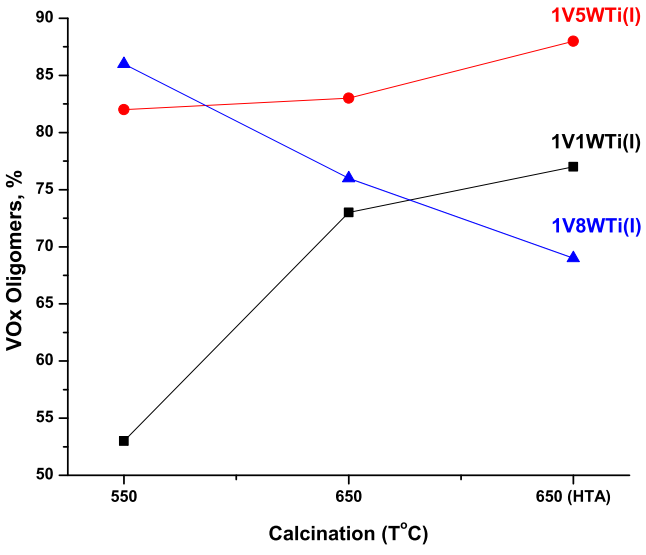

Figure 5. Percent of surface VO_x sites present as oligomers as a function of thermal treatments. Values at 550 °C for the 1V1WTi and 1V8WTi catalysts are estimated by extrapolation from comparable catalysts reported in ref 5.

Although the ^{51}V MAS NMR spectra of the dehydrated supported 1V1WTi and 1V8WTi catalysts calcined at 550 °C were not recorded, the % oligomer for these catalysts could be estimated from the corresponding 1VTi-550 °C, 1V3WTi-350 °C, and 1V5WTi-550 °C catalysts since the % of surface VO_x oligomers was found to smoothly vary with WO_x loading.[5] Increasing the calcination temperature to 650 °C increases the percent of oligomeric surface sites for the 1V1WTi catalyst, minimally affects the oligomeric fraction of surface VO_x sites for the 1V5WTi catalyst, and decreases the extent of surface VO_x oligomers for the 1V8WTi catalyst. For the catalysts HTA at 650 °C, the percent of oligomeric surface VO_x modestly increases for 1V1WTi and 1V5WTi catalysts but decreases for the 1V8WTi catalyst. The overall trends are that the extent of oligomerization of the surface VO_x sites increases with harsher thermal treatment for the 1V1WTi and 1V5WTi catalysts, but the extent of oligomerization of the surface VO_x sites decreases with harsher thermal treatment for the 1V8WTi catalyst.

3.5. *In Situ* EPR Spectroscopy of Paramagnetic Reduced V^{4+} Sites. Although solid-state ^{51}V MAS NMR spectroscopy can only detect V^{5+} sites, paramagnetic reduced V^{4+} sites in the supported V_2O_5–WO_3/TiO_2 catalysts can be detected with EPR spectroscopy. The *in situ* EPR spectra of the supported VWTi catalysts are presented in Figure 6. Analysis of all V^{4+} spins in the catalysts, which represents 95% of the total EPR signal, reveals a relatively narrow feature for the supported 1V1WTi catalysts that broadens at higher tungsten oxide content. This superposition of broad spectral features over the narrow ones is indicative of V^{4+} spins that are spatially close (oligomerized sites). The EPR signal for Ti^{3+} species was also detected (see Figure S2) but was very small relative to the V^{4+} EPR signal. An EPR signal for W^{5+} was not detected in agreement with previous findings for VWTi SCR catalysts (see Figure S2).[45] Samples containing larger quantities of tungsten oxide demonstrate an increase of another signal (evidenced by sharp features at ∼3300 G, g-value ∼2.007). A sharp feature is also present in the EPR spectra (see Figure S2), and its narrow nature renders its abundance well beneath 5% of the total EPR signal. This feature has been previously ascribed to superoxide (O_3^-, O_2^-, or O^-) species on partially reduced oxide centers.[44] There have been attempts to identify the location of these superoxide species on SCR catalytic systems by superhyperfine or pulsed EPR (ESEEM or HYSCORE), but their relationships with specific cations (V, W, and Ti) have still to be resolved.[44] It does seem from the literature as though the higher levels of superoxide signals are formed by the combination of WO_x and VO_x with the TiO_2 support (VWTi ≫ WTi ∼ Ti ≫ VTi, with no EPR signal from VTi), suggesting that the superoxides are associated with the titania sites. It must be kept in mind that the EPR measurements were conducted at −148 °C, a temperature far removed from SCR reaction conditions where the populations of V^{4+} sites may dynamically respond to the reaction environment. This would especially be true for surface V^{4+} sites, but less so for V^{4+} sites dissolved in the bulk lattice of TiO_2 (rutile) that should respond more sluggishly. An EPR signal for W(5+) sites was not detected in agreement with previous findings for VWTi SCR catalysts.[45] The ERP signal for Ti(3+), however, was detected (see Figure S2) but was very small relative to the V(4+) EPR signal.

Quantitative EPR analysis of the supported V_2O_5–WO_3/TiO_2 catalysts calcined at 550 °C previously found that the V^{4+} sites are minimal and account for no more than 1% of the total vanadium in the catalysts.[7] In contrast, the supported VWTi

https://doi.org/10.1021/acscatal.1c02130
ACS Catal. 2021, 11, 12096−12111

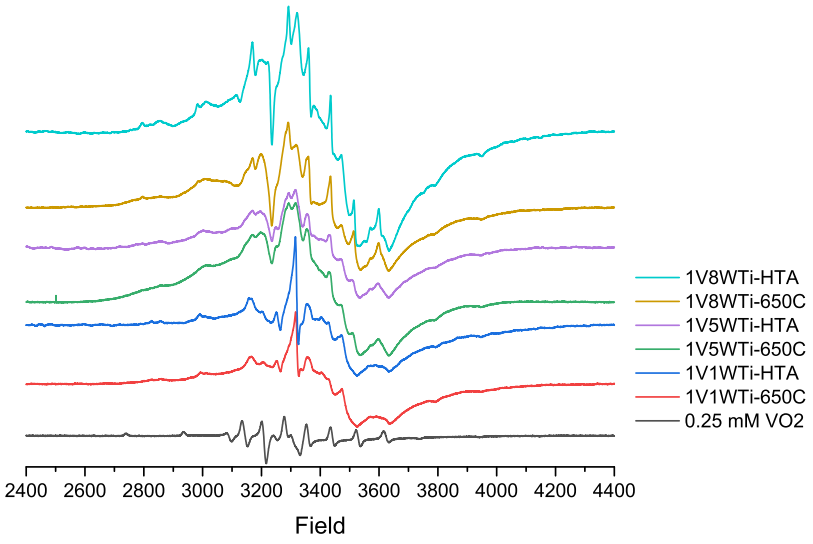

Figure 6. *In situ* EPR spectra of dehydrated supported V_2O_5–WO_3/TiO_2 catalysts calcined at 650 °C and HTA at 650 °C for 50 h. Catalysts dehydrated in air at 400 °C in flowing dry air and all samples were held in the magnet at −148 °C during spectral acquisition.

catalysts exposed to the harsher calcination and hydrothermal treatments at 650 °C possess 7−16% V^{4+} of the total vanadium (see Table S3). EPR spectroscopy is a bulk technique that is not readily able to distinguish between surface and bulk V^{4+} sites in the catalysts with the surface contribution being minor relative to the overall signal from the catalysts. It was earlier reported that the surface V^{4+} sites readily oxidize to surface V^{5+} sites in oxidizing environments at elevated temperatures.[46] Note that the catalysts were dehydrated in dry air at elevated temperatures prior to EPR analysis at −148 °C. Thus, it is most likely that the EPR V^{4+} signals are associated with the formation of the well-known $Ti_{2-x}V_xO_2$ (rutile) solid solution phase.[47,48] Formation of the $Ti_{2-x}V_xO_2$ (rutile) solid solution phase occurs because of the similar size of the V^{4+} and Ti^{4+} cations.[28] The bulk TiO_2 (rutile) phase is present in the initial TiO_2 (P-25) support, and the harsh treatments at 650 °C facilitate migration of surface VO_x sites into the TiO_2 (rutile) phase, which is accompanied by reduction of V^{5+} to V^{4+} to accommodate the vanadia in the rutile lattice. Interestingly, the hydrothermally treated catalysts contained somewhat less V^{4+} sites than their corresponding calcined catalysts. This suggests that the hydrothermal treatment environment can better retain surface $V^{5+}O_x$ sites on the titania support, which may possibly be related to the presence of steam during the hydrothermal treatment. The somewhat higher V^{4+} concentration for the 650 °C calcined 1V5WTi and 1V8WTi catalysts is probably a consequence of the higher SSA BET surface area of these catalysts that provide a greater interfacial area because of the stabilization by the surface WO_x sites that in turn allows for greater migration of V^{4+} into the TiO_2 (rutile) lattice. Importantly, the EPR measurements indicate that the formation of V^{4+} already occurs after the high-temperature calcination treatment at 650 °C prior to the hydrothermal treatment at 650 °C.

The V^{3+} sites are not detectable by either EPR or ^{51}V NMR. The presence of V^{3+} sites would have a more dramatic effect on the observation of V^{5+} sites than V^{4+} sites by NMR and EPR, respectively. Paramagnetic V^{4+} sites impact the detectability of V^{5+} sites with NMR due to broadening,[49] where up to 70% of V^{5+} within 10 Å of a V^{3+} center was previously shown to be not detected.[50] This impact could be amplified by the presence of direct V^{3+}−O−V^{5+} and V^{4+}−O−V^{5+} bonds present in surface VO_x oligomers. The concentration of V^{3+} sites, however, should be exceedingly small since there is molecular O_2 in the reactant stream after dehydration and during SCR.[51]

The EPR Ti^{3+} background signal from both the calcined and HTA V-free titania support is very small as shown in Figure S2. The EPR Ti^{3+} signal does overlap with the EPR signal for V^{4+}, but the former gives a quite narrow peak, while the latter yields relatively broad features. To further check for the possible presence of Ti^{3+} sites, a power-saturation EPR spectrum of one of the HTA vanadia catalyst samples was also collected. By saturating the V^{4+} signal, features from Ti^{3+} should become readily observable if present as a significant feature. This procedure did not yield a Ti^{3+} EPR signal but did confirm the presence of two V^{4+} signals. As such, the EPR peak areas should represent the V^{4+} content in the catalysts.

3.6. *In Situ* IR Spectroscopy of Adsorbed Ammonia Species. The nature of the adsorbed ammonia species on the dehydrated supported V_2O_5–WO_3/TiO_2 catalysts was determined with temperature-programmed *in situ* IR (TP-IR) spectroscopy. Surface NH_3^* species on Lewis acid sites vibrate at 1206 (s), 1605 (m), and 3250 (w) cm^{-1} and surface NH_4^{+}* species on Brønsted acid sites vibrate at 1425 (s), 1656 (m), 2808 (vw), 3050 (vw), and 3400 (m) cm^{-1}. The integrated IR bands of the surface NH_3^* species (1206 cm^{-1}) and surface NH_4^{+}* species (1425 cm^{-1}) after ammonia adsorption at 110 °C are presented in Figure 7, and the original IR spectra are shown in Figure S3. It was demonstrated in an earlier study that the relative IR sensitivities for surface NH_3^*/NH_4^{+}* species is ∼1 for the present spectrometer.[39]

The TiO_2 support possesses only surface NH_3^* species on Lewis acid sites,[39,52,53] and introduction of surface VO_x and WO_x sites onto the TiO_2 support always decreases the number of surface NH_3^* on Lewis acid sites and increases the number of surface NH_4^{+}* on Brønsted acid sites (see intensity of IR signals at 110 °C). The decrease in the number of Lewis acid sites with increasing surface VO_x/WO_x coverage reflects the anchoring of these surface metal oxides at the surface Lewis acid sites of the TiO_2 support.[54] Consequently, the number of Lewis acid sites decreases with increasing surface VO_x/WO_x coverage (1V1WTi > 1V5WTi > 1V8WTi at 110 °C). The

https://doi.org/10.1021/acscatal.1c02130
ACS Catal. 2021, 11, 12096−12111

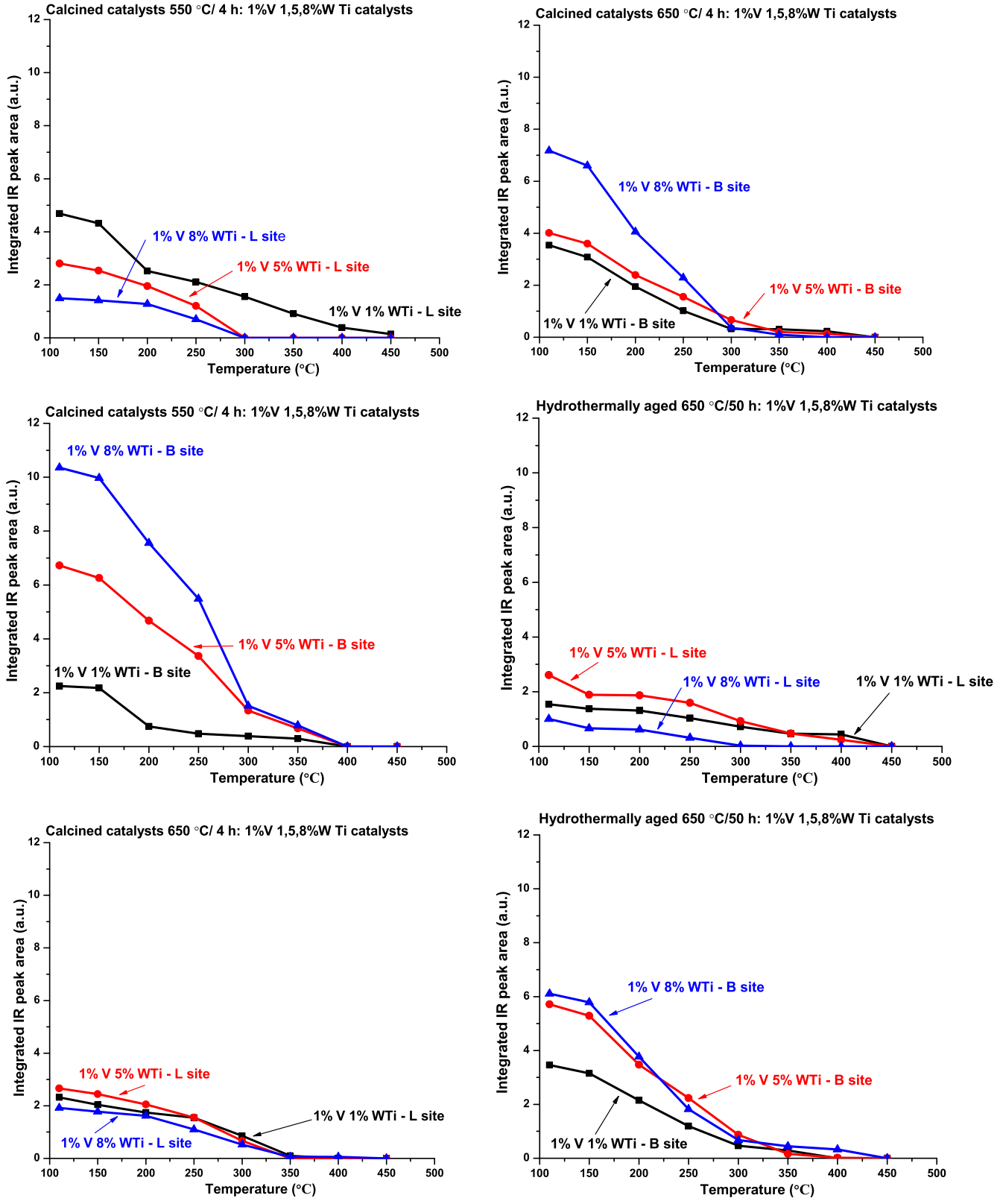

Figure 7. Number of surface NH_3^* (1206 cm^{-1}) and NH_4^{+*} (1425 cm^{-1}) species on titania-supported V_2O_5–WO_3 catalysts determined with *in situ* IR TPSR of adsorbed ammonia in flowing NO/O_2 for the catalysts calcined at 550 and 650 °C and HTA at 650 °C. The intensity of the IR bands from the surface ammonia species is normalized with respect to the IR band of the TiO_2 support at ~940 cm^{-1}.

corresponding increase in the number of Brønsted acid sites with increasing surface VO_x/WO_x coverage indicates that the Brønsted acid sites are associated with the surface VO_x/WO_x sites on the TiO_2 support. As a result, the number of Brønsted acid sites increases with increasing surface VO_x/WO_x coverage (1V1WTi < 1V5WTi < 1V8WTi at 110 °C). The Brønsted acid sites have been proposed to be located at bridging V–$(OH)^+$–Ti and W–$(OH)^+$–Ti sites.[9,39,52] The number of

https://doi.org/10.1021/acscatal.1c02130
ACS Catal. 2021, 11, 12096−12111

surface Lewis and Brønsted acid sites is also strongly dependent on the thermal pretreatments, especially when the severity of the pretreatment is increased (calcination at 550 °C < calcination at 650 °C < hydrothermal aging at 650 °C). Increasing the severity of the pretreatment generally decreases the number of surface Lewis acid sites at 110 °C because the number of exposed surface Lewis acid sites from the TiO_2 support diminishes, which is a consequence of the decreasing surface area of the titania support and increasing surface VO_x and WO_x coverage. The number of surface NH_3^* species on Lewis acid sites at 110 °C is dramatically diminished for the most aggressive hydrothermal treatment at 650 °C, while the number of surface NH_4^+* species on Brønsted acid sites at 110 °C is almost insensitive to the severity of the pretreatment. These trends indicate that the ratio of surface NH_4^+*/NH_3^* species, Brønsted/Lewis acid sites, increases with pretreatment severity for unpromoted supported V_2O_5–WO_3/TiO_2 catalysts.

The reactivity of surface NH_3^* species on Lewis acid sites and surface NH_4^+* species on Brønsted acid sites for the calcined and HTA-supported V_2O_5–WO_3/TiO_2 catalysts in the presence of flowing NO/O_2 was probed with temperature-programmed *in situ* IR (TP-IR) spectroscopy and the results are presented in Figures 7 and S3. For the catalysts calcined at 550 °C, the surface NH_3^* species react or desorb at 300 °C for higher tungsten oxide loading, while the surface NH_4^+* species react or desorb at 400 °C. For the catalysts calcined at 650 °C, the surface NH_3^* species react or desorb by 425 °C, while the surface NH_4^+* species react or desorb at 300–400 °C. While the reactivity or desorption of the surface NH_3^* species is independent of tungsten oxide loading, the reactivity or desorption of the surface NH_4^+* decreases with tungsten oxide loading. For the catalysts HTA at 650 °C, the number of surface NH_3^* species sites has been dramatically reduced, and the surface NH_4^+* species react or desorb between 250 and 425 °C. The reactivity or desorption of the surface NH_4^+* decreases with tungsten oxide loading and generally increases with severity of treatment. The reactivity or desorption trends during temperature programming in flowing NO/O_2 indicate that surface NH_4^+*species are slightly more stable on supported VWTi catalysts than surface NH_3^* species.

3.7. Steady-State SCR Activity and TOF Values. The steady-state SCR activity and TOF values of the supported 1% V_2O_5–$x$$WO_3/TiO_2$ catalysts calcined at 550 °C, calcined at 650 °C, and hydrothermally treated at 650 °C are presented in Figure 8. Both the steady-state activity and TOF values [normalized by the total V sites in each catalyst as given in Table S1, which neglects the small fraction of V dissolved in the TiO_2 (rutile) phase as $Ti_{1-x}V_xO_2$] tracked each other as a function catalyst composition and thermal treatments. Increasing the tungsten oxide loading always increased the catalyst performance for the same thermal treatment. While the TOF for the supported 1% V_2O_5–1% WO_3/TiO_2 catalyst slightly increased with calcination at 650 °C, the TOF values for the supported 1% V_2O_5–5% WO_3/TiO_2 and 1% V_2O_5–8% WO_3/TiO_2 catalysts decreased with calcination at 650 °C. The SCR catalytic activity and TOF values for each catalyst did not change significantly in going from calcination at 650 °C to hydrothermal treatment at 650 °C.

3.8. Correlation Plots. The above characterization and SCR activity data were organized as a radar plot that allows comparing the relationships among multiple catalyst variables with the distance from the center representing the intensity of the specific property, as shown in Figure 9 for the set of nine supported 1% V_2O_5–x% WO_3/TiO_2 catalysts. The red curve represents the SCR catalytic activity plot. The radar plot shape indicates that the strongest relationship exists between the SCR catalytic activity and the number of surface Brønsted acid sites (yellow curve). A relationship between the SCR catalytic activity and number of Lewis acid sites (green curve) does not exist, and, consequently, only a moderate relationship is present between the SCR catalytic activity and the total number of surface Lewis and Brønsted acid sites (purple curve). The relationships between the SCR activity and the BET surface area (grey curve) and fraction of oligomeric surface vanadia sites (orange curve) are also not apparent. The individual correlation plots between the SCR activity and each

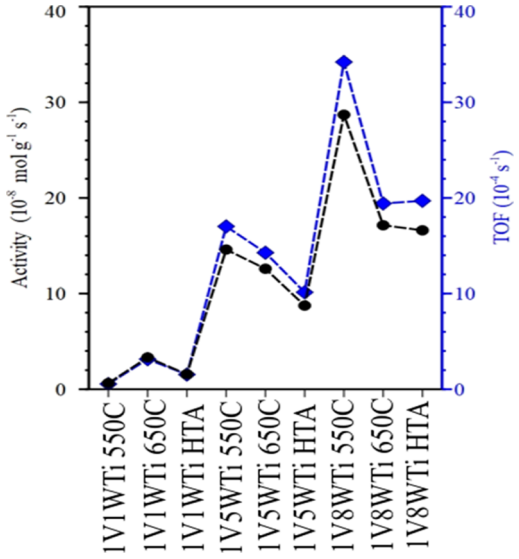

Figure 8. Steady-state SCR activity and TOF values at 200 °C for 550 °C calcined, 650 °C calcined, and 650 °C HTA-supported 1% V_2O_5–x% WO_3/TiO_2 catalysts. The TOF values were calculated by dividing the activity rates by the total number of V sites in each catalyst as given in Table S1.

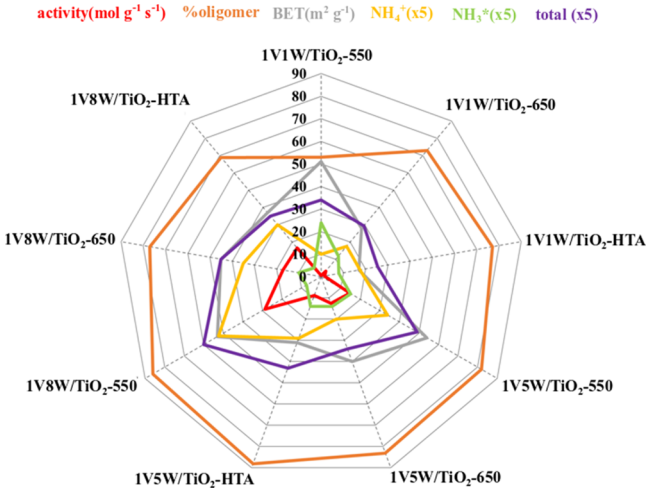

Figure 9. Radar plot of catalytic activity and catalyst properties number of Lewis acid sites (NH_3^*), number of Brønsted acid sites (NH_4^+*), total number of acid sites (Lewis and Brønsted), BET surface area, BET surface area, and fraction of surface vanadia oligomers.

https://doi.org/10.1021/acscatal.1c02130
ACS Catal. 2021, 11, 12096–12111

catalyst parameter are shown in Figures S4 and S5 and include correlation coefficients which confirm the conclusions arrived at from the radar plot. Moreover, individual radar plots are also shown in Figure S5, as a function of treatment (Figure S5a−c), and as a function of W loading (Figure S5d−f).

4. DISCUSSION

4.1. Bulk Structures of Calcined and HTA-Supported V_2O_5−WO_3/TiO_2 Catalysts. The only bulk structures present in the calcined and HTA-supported 1% V_2O_5−x% WO_3/TiO_2 catalysts are the TiO_2 (anatase) and TiO_2 (rutile) phases of the titania support (see Figure 1 and Table S2). The detection of a TiO_2 (rutile) shell layer on a TiO_2 (anatase) core was surprisingly detected for the most severely transformed supported 1V1WTi catalyst and represents a new catalyst deactivation mechanism that was not previously observed. This core/shell structure may also be present in the HTA-supported 1V5WTi and 1V8WTi catalysts, but the much stronger TiO_2 (anatase) Raman bands from these catalysts may overshadow the much weaker TiO_2 (rutile) Raman bands. The rutile phase is also able to incorporate V^{4+} cations into its bulk lattice [$Ti_{1-x}V_xO_2$ (rutile)].[28] The presence of the V^{4+} cations in the 650 °C calcined and HTA catalysts is directly confirmed by the *in situ* EPR spectroscopy measurements (see Figure 5). The V^{4+} EPR measurements, however, detect the V^{4+} sites in the catalysts and are dominated by the contribution of the V^{4+} sites present in the bulk $Ti_{1-x}V_xO_2$ (rutile) solid solution related to the ∼20% TiO_2 (rutile) phase present in the starting titania support as well as the additional TiO_2 (rutile) formed from the treatments at 650 °C. The formation of the additional TiO_2 (rutile) phase is retarded with increasing surface tungsten oxide coverage (see Table S2). Incorporation of as much as 6−16% of V as $V^{4+}O_2$ into the $Ti_{1-x}V_xO_2$ (rutile) lattice was found, with the amount of $V^{4+}O_2$ increasing with harsher thermal treatments and tungsten oxide loading (see Table S3). The amount of dissolved bulk V^{4+} cations appears to track the BET surface area of the TiO_2 support and not the fraction of bulk TiO_2 (rutile) phase, suggesting that higher BET surface area allows for a greater opportunity of surface VO_x to diffuse into the bulk TiO_2 (rutile) phase. The hydrothermal treatment, unexpectedly, decreased the amount of dissolved V^{4+} cations. This may reflect stabilization of the surface VO_x sites by the moist environment by maintaining the surface VO_x as V^{5+} cations that cannot dissolve into the TiO_2 (rutile) lattice. Crystalline V_2O_5 and WO_3 nanoparticles are absent from the investigated catalysts (see Figure 2). Higher thermal treatment temperatures (>680 °C) typically result in the formation of crystalline V_2O_5 and WO_3 nanoparticles as the decreases in BET surface area (see Table S1) result in decreased available anchoring sites for the surface VO_x and WO_x sites on the TiO_2 support, which leads to the transformation of surface VO_x and WO_x sites to crystalline V_2O_5 and WO_3 nanoparticles.[15,16]

4.2. Surface Structures of Calcined and HTA-Supported V_2O_5−WO_3/TiO_2 Catalysts. The titania-supported vanadium oxide and tungsten oxide phases are primarily present as surface sites anchored onto the TiO_2 support as revealed by Raman (see Figure 2) and HS-LEIS (see Figure 3). The surface VO_x and WO_x sites are present as isolated and oligomeric mono-oxo VO_x and mono-oxo WO_x sites with the extent of oligomerization increasing with surface VO_x and WO_x coverage on the TiO_2 support for the catalysts calcined at 550 °C.[5] The oligomerization of surface VO_x sites with increasing surface VO_x coverage and in the presence of surface WO_x sites is a structural effect related to the crowding, or formation of surface islands, of the surface VO_x sites on the TiO_2 support that is induced by the decreased number of anchoring sites available for the surface VO_x sites in the presence of surface WO_x sites. The 1V1WTi catalyst undergoes the most dramatic increase in the fraction of oligomeric surface VO_x sites with increasing harshness of the thermal treatment (calcination at 550 °C < calcination at 650 °C < hydrothermal aging at 650 °C), while the 1V5WTi catalyst undergoes a modest increase in the fraction of oligomeric surface VO_x sites with increasing harshness of the thermal treatment. The increase of the fraction of oligomeric surface VO_x sites is related to the higher surface coverage of the VO_x and WO_x sites on the TiO_2 support with increasingly harsher thermal treatments brought about by the shrinking of the titania support surface area (see Table 1 and Figures 4, 5, and S1). In contrast, the fraction of oligomeric surface VO_x sites for the 1V8WTi catalyst decreases with increasing harshness of the thermal treatment. The origin of this different trend with increasing harshness of the thermal treatment is currently not understood. It may result from the higher BET surface area of the 1V8WTi catalysts that allows for enhanced diffusion of VO_x into the TiO_2 (rutile) bulk lattice and may also be taking place for the 1V1WTi and 1V5WTi catalysts but is masked by the more pronounced decreases in the surface area of these catalysts with thermal treatments responsible for oligomerization of the surface VO_x sites. The concentration of the surface VO_x sites is only slightly decreased by the thermal treatments at 650 °C (8−16%), as mentioned above, due to vanadia incorporation into the TiO_2 (rutile) lattice as $V^{4+}O_2$ (see Table S3) and should not have a significant effect on the fraction of oligomeric surface VO_x sites. The surface WO_x sites should not be affected by dissolution into the TiO_2 (rutile) phase because the titania bulk lattice, consisting of Ti^{4+} sites, is not able to accommodate the larger charge of the W^{6+} cation. Some surface WO_x may have volatized under the more extreme thermal treatment conditions, but the tungsten oxide content of the catalysts were not analyzed. The surface VO_x and WO_x, thus, are the predominant sites on the outermost surface layer of the TiO_2 support with only minor amounts of VO_x lost by dissolution and volatilization under the conditions examined in the present study.

4.3. Influence of Calcination and Hydrothermal Aging on Surface Acidity of Supported V_2O_5−WO_3/TiO_2 Catalysts. Both surface NH_3^* species on Lewis acid sites and surface NH_4^+* species on Brønsted acid sites are typically present on the supported V_2O_5−WO_3/TiO_2 SCR catalysts. The presence of both of these surface intermediates on the catalyst has resulted in a long-standing debate as to which adsorbed ammonia species plays a key role in the SCR reaction.[16,27,55−57] Some studies have proposed that the surface NH_3^* species implicate the Lewis acid sites as the catalytic active sites for the SCR reaction while others have proposed that the surface NH_4^+* species implicate the Brønsted acid sites as the catalytic active sites. A major complication in these studies is that both surface NH_3^* and surface NH_4^+* species are simultaneously present and that moisture also converts the former to the latter under SCR reaction conditions above ∼225 °C.[39] Surprisingly, the 650 °C hydrothermally treated supported catalysts primarily possess surface NH_4^+* species on Brønsted acid sites (see Figures 7 and S2) allowing us to address this issue. The lower concentration of surface NH_3^* species on Lewis acid sites,

https://doi.org/10.1021/acscatal.1c02130
ACS Catal. 2021, 11, 12096−12111

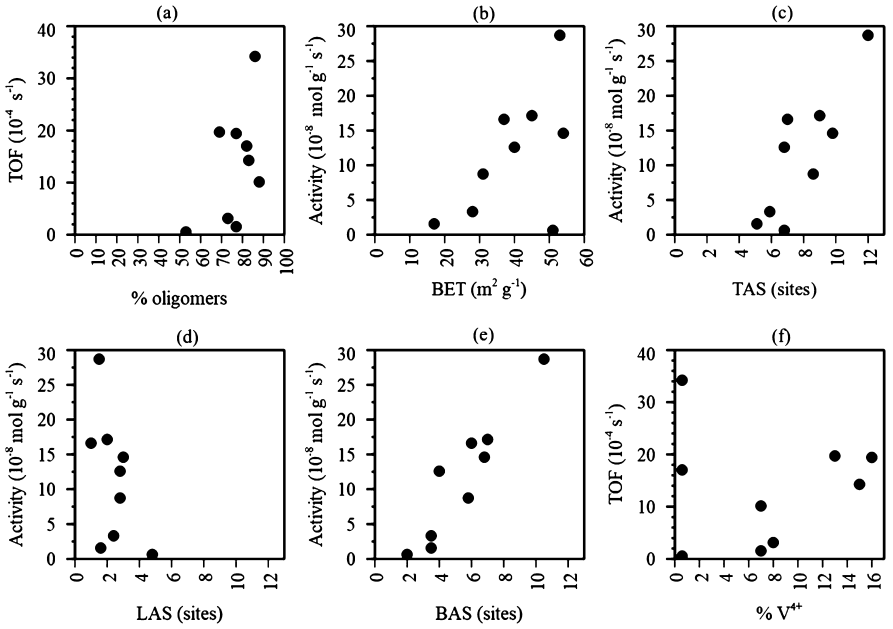

Figure 10. Correlation plots between steady-state SCR TOF values at 200 °C and structural properties of the series of supported VWTi catalysts: (a) surface VO_x oligomer sites (%), (b) BET (m^2/g), (c) total number of adsorbed ammonia species, (d) number of surface NH_3^* species, (e) number of surface NH_4^{+}* species, and (f) V^{4+} sites (%).

however, has only a minor effect on the SCR activity as shown by comparison of catalysts calcined at 650 °C, containing both types of surface ammonia species, and catalysts HTA at 650 °C that contain primarily surface NH_4^{+}* species (see Figures 7 and 8). The present finding suggests that surface NH_4^{+}* species on Brønsted acid sites, primarily associated with the surface VO_x sites,[27] are able to efficiently perform the SCR reaction for the catalysts in the current study.

In contrast to the present findings, Marberger *et al.*[15,16,27] observed the presence of both surface NH_3^* and NH_4^{+}* species on their hydrothermally treated catalysts and that the concentration of surface NH_3^* species preferentially diminished when NO/O_2 was introduced. It should be noted, however, that there are several experimental differences between the present studies and those reported by Marberger *et al.* The TiO_2 support employed by Marberger possessed ~100 m^2/g and was present as 100% TiO_2 (anatase). The hydrothermal treatments employed in the Marberger *et al.* investigation consisted of 10% H_2O while in the present study a mixture of 8% H_2O, 10% O_2, 7% CO_2, and 75% N_2 was used for the hydrothermal aging, but this would not be expected to contribute a significant difference. More importantly, Marberger *et al.* coated their catalysts on a monolith, which initially contained surface sulfates that desorbed during the hydrothermal treatment and possible presence of other unreported additives or impurities. The TiO_2 (P-25) support used in the present study is known to be extremely free of impurities and has ~55 m^2/g with an initial ~80/20 anatase/rutile mixture. The major significant difference between the catalysts studied by Marberger *et al.* and the present study may be the presence of surface impurities in the Marberger *et al.* investigation. Furthermore, surface NH_3^* species on the surface VO_x sites readily transform to surface NH_4^{+}* species in the presence of moisture above ~225 °C.[39] It is important that studies from different labs compare the same V_2O_5–WO_3/TiO_2 catalyst system to determine if the variable reports are related to the different catalysts employed, synthesis methods, or the reaction conditions. It is suggested that reference studies should always be performed with the very clean TiO_2 (P-25) since this is a standard TiO_2 support widely used in catalysis studies.

4.4. Influence of Calcination and Hydrothermal Aging on Structure–Activity Relationships for SCR of Supported V_2O_5–WO_3/TiO_2 Catalysts. The supported VWTi catalysts calcined at 550 °C consist of surface VO_x and WO_x sites on the TiO_2 support and the SCR activity depends on the extent of oligomerization of the surface VO_x sites since the SCR reaction requires two adjacent VO_x sites.[5] The oligomerization of surface VO_x sites increases with surface VO_x coverage as well as surface WO_x coverage. For the supported 1V1–8WTi catalysts calcined at 550 °C that have similar vanadia loading, thus, the TOF strongly increases with surface tungsten oxide coverage (see Figure 8). Calcination at 650 °C and hydrothermal treatments at 650 °C resulted in several simultaneous structural changes: (1) decrease in BET surface area- (see Table 1), (2) increase in surface density of VO_x and WO_x sites, (3) increase in fraction of oligomeric surface VO_x sites for 1V1WTi and 1V5WTi, but not for 1V8WTi (see Figure 5), (4) change in the distribution of surface NH_3^* and NH_4^{+}* species (see Figure 7), (5) transformation of a portion of TiO_2 (anatase) into TiO_2 (rutile) (see Table S2), and (6) dissolution of minor amounts of vanadia (V^{4+}) into the TiO_2 (rutile) bulk lattice (see Table S3).[28] To try to better understand the impact of these structural changes on SCR activity, correlation plots between these structural changes and the SCR TOF values are presented in Figures 10a–f and S3a–f. Recall that both SCR activity and TOF values followed tracked each other where TOF was determined by normalizing against the total vanadia in the catalysts. Although the fraction of oligomeric surface VO_x sites is a good predictor of SCR activity for catalysts calcined at 550 °C, several additional structural changes take place with calcination and hydrothermal treatments at 650 °C that make for a more complex situation. For example, the TOF/activity values for the supported 1V5WTi catalyst

https://doi.org/10.1021/acscatal.1c02130
ACS Catal. 2021, 11, 12096–12111

decrease with the severity of thermal treatment, but the fraction of oligomeric surface VO_x sites modestly increases, indicating that other factors must also contribute to the overall outcome, which may be overshadowing the relationship between fraction of oligomeric surface VO_x sites and TOF as shown in Figures 10a and S3a. There is no correlation between TOF/activity values and BET surface areas since as the surface area decreases from 1V1WTi (calcined 550 °C) to1V1WTi (calcined at 650 °C) as shown in Figures 10b and S3b. The TOF value increases mainly due to the significant increase in the concentration of oligomeric surface VO_x sites (see Figures 10a and S3a). There is a correlation between TOF/activity values and the total amount of surface NH_3^* and NH_4^{+}* species as shown in Figures 10c and S3c. This may not be surprising since the surface NH_3^* and NH_4^{+}* species are the surface reaction intermediates on the catalytic active sites. The variation in TOF/activity values does not correlate with the amount of surface NH_3^* species since the TOF value continuously decreases for the supported 1V5WTi catalyst, while the surface concentration of NH_3^* initially increases and then decreases as shown in Figures 10d and S3d. The amount of surface NH_4^{+}* species does, however, vary in tandem with the TOF/activity values (see Figures 10e and S3e). The combined amounts of surface NH_3^* and NH_4^{+}* species also vary in tandem with the SCR TOF values as shown in Figures 10c and S3c because there are many more surface NH_4^{+}* species than surface NH_3^{+}* species in these catalysts (see Figure 10d,e). Removal of a small amount of surface VO_x sites by formation of dissolved V^{4+} cations also does not correlate with the TOF/activity values as shown in Figures 10f and S3f since as the fraction of bulk V^{4+} for the 1V5WTI catalyst decreases, the TOF/activity values decrease.

Although the simultaneous contributions from multiple catalyst variables during the hydrothermal treatments make it difficult to completely understand the catalyst structure−activity relationships, there are some trends present in the correlation plots of Figures 9, 10, and S3. The SCR TOF/activity correlates with the total number of surface ammonia on acid sites that is dominated by the surface NH_4^{+}* species on Brønsted acid sites. The reason for this is that the surface ammonia species are chemically probing the surface acid sites involved in the SCR reaction. The SCR TOF/activity does not correlate with the BET specific surface area, fraction of TiO_2 (rutile) phase, and dissolved V^{4+} in the rutile lattice. The BET-specific surface area is a textural parameter that does not provide information about the nature of the catalytic active sites and, therefore, cannot correlate with the SCR TOF/activity. The fraction of TiO_2 (rutile) does not correlate with the SCR TOF/activity since this is a bulk parameter and does not reflect the situation at the catalyst surface. Even though the TiO_2 (rutile) phase is able to dissolve some V^{4+} sites, the removal of the minor amount of surface VO_x at 650 °C does not have a significant impact on the overall SCR TOF/activity.

An interesting finding is that the SCR performance of the supported VWTi catalysts is only minimally degraded when going from calcination at 650 °C, representative of a freshly activated catalyst, to extended hydrothermal aging at 650 °C, representative of a working used catalyst. This is because most of the catalyst surface structural and surface chemical changes already occur upon calcination at 650 °C. Calcination or hydrothermal aging at higher temperatures (>650 °C), however, intensifies the catalyst surface structural and surface chemical changes that will significantly degrade the SCR performance (*e.g.*, loss of the surface VO_x catalytic active sites by volatilization and further dissolution into the TiO_2 (rutile) bulk lattice and volatilization of the surface WO_x promoter).[15,16,27]

5. CONCLUSIONS

The hydrothermal "degreening" treatment at 650 °C of supported V_2O_5−WO_3/TiO_2 catalysts is applied in the industry to accelerate activation and aging of fresh catalysts for testing of SCR performance. Such harsh treatments significantly affect the physical and chemical properties of supported V_2O_5−WO_3/TiO_2 SCR catalysts. The hydrothermal treatments decrease the surface area of the TiO_2 support and transform a fraction of the titania support phase from TiO_2 (anatase) to TiO_2 (rutile). The TiO_2 (rutile) phase can also incorporate a small amount of V^{4+}, ∼8−16% of total vanadia, into its bulk lattice as a $Ti_{1-x}V_xO_2$ solid solution that depletes the number of surface VO_x catalytic active sites. The surface WO_x sites behave as a textural promoter that retards the negative effects from hydrothermal treatment with its presence countering the negative effects and its impact increasing with tungsten oxide loading up to monolayer coverage. Additionally, the presence of the surface WO_x sites also tends to enhance the concentration of the more active oligomerized surface VO_x sites. The ratio of surface NH_3^*/NH_4^{+}* species on Lewis and on Brønsted acid sites, respectively, decreases with the harshness of the thermal treatment, and the 650 °C HTA catalysts contain very low concentrations of surface NH_3^* species. This finding suggests that surface NH_4^{+}*, primarily associated with the surface VO_x sites, are able to efficiently perform the SCR reaction. SCR structure−activity relationships were difficult to establish since multiple structural and surface chemical properties of the catalysts were simultaneously changing during the harsh thermal treatments, which made it difficult to correlate the SCR activity with any single catalyst parameter. A correlation, however, was found between the SCR TOF/activity and the sum of the surface NH_3^* and NH_4^{+}* species, which is dominated by the surface NH_4^{+}* species. Although both surface NH_3^* species on Lewis acid sites and surface NH_4^{+}* species on Brønsted acid sites participate in the SCR reaction, the surface NH_4^{+}* species on Brønsted acid sites are the key reaction intermediates during the SCR reaction by the unpromoted V_2O_5−WO_3/TiO_2 catalysts employed in the current study. The present study also shows that SCR catalysts must be activated at high calcination temperature (650 °C) and hydrothermal treatment (650 °C) to accurately represent the state of the catalyst surface present under industrial reaction conditions that represent freshly activated catalysts and working used catalysts, respectively.

■ ASSOCIATED CONTENT

Supporting Information

The Supporting Information is available free of charge at https://pubs.acs.org/doi/10.1021/acscatal.1c02130.

ICP of vanadium content of catalysts; crystallite sizes for supported VWTi catalysts treated at 650 °C; EPR determination of V^{4+}; solid-state ^{51}V MAS NMR spectra of dehydrated supported V_2O_5−WO_3/TiO_2 catalysts calcined at 650 °C; EPR spectra of non-vanadium species; *in situ* TP-IR spectra of surface ammonia species during SCR; correlation plots between steady-state SCR TOF values and structural properties of VWTi catalysts;

https://doi.org/10.1021/acscatal.1c02130
ACS Catal. 2021, 11, 12096−12111

and radar plots of catalytic activity and catalyst properties (PDF)

AUTHOR INFORMATION

Corresponding Authors

Yong Wang − *Institute for Integrated Catalysis and Earth and Biological Science Directorate, Pacific Northwest National Laboratory, Richland, Washington 99354, United States*; Email: wang42@wsu.edu

Jian Zhi Hu − *Institute for Integrated Catalysis and Earth and Biological Science Directorate, Pacific Northwest National Laboratory, Richland, Washington 99354, United States*; orcid.org/0000-0001-8879-747X; Email: Jianzhi.Hu@pnnl.gov

Israel E. Wachs − *Operando Molecular Spectroscopy & Catalysis Laboratory, Department of Chemical & Biomolecular Engineering, Lehigh University, Bethlehem, Pennsylvania 18015, United States*; orcid.org/0000-0001-5282-128X; Email: iew0@lehigh.edu

Authors

Jun-Kun Lai − *Operando Molecular Spectroscopy & Catalysis Laboratory, Department of Chemical & Biomolecular Engineering, Lehigh University, Bethlehem, Pennsylvania 18015, United States*

Nicholas R. Jaegers − *Institute for Integrated Catalysis and Earth and Biological Science Directorate, Pacific Northwest National Laboratory, Richland, Washington 99354, United States*; orcid.org/0000-0002-9930-7672

Bar Mosevitzky Lis − *Operando Molecular Spectroscopy & Catalysis Laboratory, Department of Chemical & Biomolecular Engineering, Lehigh University, Bethlehem, Pennsylvania 18015, United States*

Mingyu Guo − *Operando Molecular Spectroscopy & Catalysis Laboratory, Department of Chemical & Biomolecular Engineering, Lehigh University, Bethlehem, Pennsylvania 18015, United States*

Michael E. Ford − *Operando Molecular Spectroscopy & Catalysis Laboratory, Department of Chemical & Biomolecular Engineering, Lehigh University, Bethlehem, Pennsylvania 18015, United States*; orcid.org/0000-0002-0403-801X

Eric Walter − *Institute for Integrated Catalysis and Earth and Biological Science Directorate, Pacific Northwest National Laboratory, Richland, Washington 99354, United States*; orcid.org/0000-0003-3644-5514

Complete contact information is available at: https://pubs.acs.org/10.1021/acscatal.1c02130

Notes

The authors declare no competing financial interest.

ACKNOWLEDGMENTS

This work was supported as part of Understanding & Control of Acid Gas-Induced Evolution of Materials for Energy (UNCAGE-ME), an Energy Frontier Research Center funded by the U.S. Department of Energy, Office of Science, Basic Energy Sciences under Award #DE-SC0012577. The NMR and EPR research at Pacific Northwest National Laboratory (PNNL) were supported by the U.S. Department of Energy, Office of Science, Office of Basic Energy Sciences, Division of Chemical Sciences, Geosciences, and Biosciences. Experiments were conducted in the Environmental Molecular Sciences Laboratory (grid.436923.9), a DOE Office of Science User Facility located at Pacific Northwest National Laboratory (PNNL). NMR experiments were conducted using a Bruker 600 MHz NMR spectrometer acquired with support from the US Department of Energy, Office of Science, Office of Basic Energy Sciences. PNNL is a multi-program national laboratory operated by Battelle for the U.S. Department of Energy under Contract DE-AC05-76RL01830. The authors thank Sofia Liu from National Taiwan University, Taipei, for providing the TiO_2 (anatase) standard. In addition, the authors thank Dr. Henry Luftman for the HS-LEIS spectra, and Daniyal Kiani for preparation of the correlation graphs and radar plot.

REFERENCES

(1) Lietti, L.; Alemany, J. L.; Forzatti, P.; Busca, G.; Ramis, G.; Giamello, E.; Bregani, F. Reactivity of V2O5-WO3/TiO2 Catalysts in the Selective Catalytic Reduction of Nitric Oxide by Ammonia. *Catal. Today* **1996**, *29*, 143−148.

(2) Vuurman, M. A.; Wachs, I. E.; Hirt, A. M. Structural Determination of Supported V2O5-WO3/TiO2 Catalysts by in Situ Raman Spectroscopy and x-Ray Photoelectron Spectroscopy. *J. Phys. Chem.* **1991**, *95*, 9928−9937.

(3) Alemany, L. J.; Berti, F.; Busca, G.; Ramis, G.; Robba, D.; Toledo, G. P.; Trombetta, M. Characterization and Composition of Commercial V2O5-WO3- TiO2 SCR Catalysts. *Appl. Catal., B* **1996**, *10*, 299−311.

(4) Wachs, I. E.; Deo, G.; Weckhuysen, B.; Andreini, A.; Vuurman, M.; de Boer, M.; Amiridis, M. Selective Catalytic Reduction of NO with NH 3 over Supported Vanadia Catalysts. *J. Catal.* **1996**, *161*, 211−221.

(5) Jaegers, N. R.; Lai, J. K.; He, Y.; Walter, E.; Dixon, D. A.; Vasiliu, M.; Chen, Y.; Wang, C.; Hu, M. Y.; Mueller, K. T.; et al. Mechanism by Which Tungsten Oxide Promotes the Activity of Supported V 2 O 5 / TiO 2 Catalysts for NO X Abatement : Structural Effects Revealed by 51 V MAS NMR Spectroscopy Research Articles. *Angew. Chem., Int. Ed.* **2019**, *58*, 12609−12616.

(6) Lai, J.-K.; Wachs, I. E. A Perspective on the Selective Catalytic Reduction (SCR) of NO with NH3 by Supported V2O5 −WO3/TiO2 Catalysts. *ACS Catal.* **2018**, *8*, 6537−6551.

(7) Chen, J. P.; Yang, R. T. Selective Catalytic Reduction of NO with NH3 on SO4/TiO2 Superacid Catalyst. *J. Catal.* **1993**, *139*, 277−288.

(8) Wachs, I. E. Catalysis Science of Supported Vanadium Oxide Catalysts. *Dalton Trans.* **2013**, *42*, 11762−11769.

(9) He, Y.; Ford, M. E.; Zhu, M.; Liu, Q.; Tumuluri, U.; Wu, Z.; Wachs, I. E. Influence of Catalyst Synthesis Method on Selective Catalytic Reduction (SCR) of NO by NH3 with V2O5-WO3/TiO2 Catalysts. *Appl. Catal., B* **2016**, *193*, 141−150.

(10) Tian, H.; Ross, E. I.; Wachs, I. E. Quantitative Determination of the Speciation of Surface Vanadium Oxides and Their Catalytic Activity. *J. Phys. Chem. B* **2006**, *110*, 9593−9600.

(11) Schenk, C.; Laroo, C. *NO x Adsorber Aging on a Heavy-Duty On-Highway Diesel Engine-Part One*, SAE Technical Paper Series, 2003; Vol. *112*, pp 40−50.

(12) Auvray, X.; Grant, A.; Lundberg, B.; Olsson, L. Catalysis Science & Technology Combined Lean NO x Trap (LNT) and Selective Catalytic Reduction (SCR) Concept. *Catal. Sci. Technol.* **2019**, *9*, 2152−2162.

(13) Knafl, A.; Han, M.; Bohac, S. V.; Assanis, D. N.; Szymkowicz, P. G. *Comparison of Diesel Oxidation Catalyst Performance on an Engine and a Gas Flow Reactor*, SAE Technical Paper 2007-01-0231, 2007; pp 1−13.

(14) Kamasamudram, K.; Currier, N. W.; Chen, X.; Yezerets, A. Overview of the Practically Important Behaviors of Zeolite-Based Urea-SCR Catalysts , Using Compact Experimental Protocol. *Catal. Today* **2010**, *151*, 212−222.

(15) Marberger, A.; Elsener, M.; Nuguid, R. J. G.; Ferri, D.; Kröcher, O. Applied Catalysis A , General Thermal Activation and Aging of a V205 / WO3-TiO2 Catalyst for the Selective Catalytic Reduction of NO with NH3. *Appl. Catal., A* **2019**, *573*, 64−72.
(16) Marberger, A.; Elsener, M.; Ferri, D.; Kröcher, O. VOx Surface Coverage Optimization of V2O5/WO3-TiO2 SCR Catalysts by Variation of the V Loading and by Aging. *Catalysts* **2015**, *5*, 1704−1720.
(17) Madia, G.; Elsener, M.; Koebel, M.; Raimondi, F.; Wokaun, A.; Raimondi, F.; Wokaun, A. Thermal Stability of Vanadia-Tungsta-Titania Catalysts in the SCR Process. *Appl. Catal., B* **2002**, *39*, 181−190.
(18) Madia, G.; Elsener, M.; Koebel, M.; Raimondi, F.; wokaun, A. Thermal Stability of Vanadia-Tungsta-Titania Catalysts in the SCR Process. *Appl. Catal., B* **2002**, *39*, 181−190.
(19) Kim, J. Y.; Cheng, Y.; Patterson, J. E.; Laing, P. M.; Lambert, C. K. *Modeling Study of SCR Catalyst Aging Characteristics*, SAE Technical Paper, 2007-01-15802, 2007.
(20) Maunula, T.; Kinnunen, T.; Kanniainen, K.; Viitanen, A.; Savimaki, A. *Thermally Durable Vanadium SCR Catalysts for Diesel Applications*, SAE Technical Paper, 2013-01-1063, 2013.
(21) Girard, J. W.; Montreuil, C.; Kim, J.; Cavataio, G.; Lambert, C. Technical Advantages of Vanadium SCR Systems for Diesel NOx Control in Emerging Markets. *SAE Int. J. Fuels Lubr.* **2008**, *1*, 488−494.
(22) Chapman, D. M.; Fu, G.; Augustine, S.; Crouse, J.; Zavalij, L.; Watson, M.; Perkins-Banks, D. New Titania Materials with Improved Stability and Activity for Vanadia-Based Selective Catalytic Reduction of NOx. *SAE Int. J. Fuels Lubr.* **2010**, *3*, 643−653.
(23) Asako, T.; Kai, R.; Toyoshima, T.; Vogt, C.; Hirose, S.; Nakao, S. *Evaluation of Hydrothermally Aged Vanadia SCR on High Porosity Substrate*, SAE Technical Paper, 2016-01-2320, 2016.
(24) Maunula, T.; Kinnunen, T.; Iivonen, M. *Design and Durability of Vanadium-SCR Catalyst Systems in Mobile Off-Road Applications*, SAE Technical Paper, 2011-01-1316, 2011.
(25) Kababji, A.; Abhyankar, A.; Li, H.; Boopathi, S. M.; Reining, A. *Design and Durability of Vanadium-SCR Catalytic Aftertreatment System to Meet Tier 4 Emission Regulations in a Locomotive Application*, SAE Technical Paper 2019-01-5015, 2019.
(26) Maunula, T.; Viitanen, A.; Kinnunen, T.; Kanniainen, K. *Design of Durable Vanadium-SCR Catalyst Systems for Heavy-Duty Diesel Applications*, SAE Technical Paper 2013-01-0049, 2013.
(27) Marberger, A.; Ferri, D.; Elsener, M.; Kröcher, O. The Significance of Lewis Acid Sites for the Selective Catalytic Reduction of Nitric Oxide on Vanadium-Based Catalysts. *Angew. Chem., Int. Ed.* **2016**, *55*, 11989−11994.
(28) Cole, D. J.; Cullis, C. F.; Hucknall, D. J. Studies of Heterogeneous Oxidation Catalysts. Part 1. The Vanadium(V) Oxide + Titanium(IV) Oxide system. *J. Chem. Soc., Faraday Trans. 1* **1976**, *72*, 2185−2196.
(29) Routray, K.; Deo, G. Kinetic Parameter Estimation for a Multiresponse Nonlinear Reaction Model. *AIChE J.* **2005**, *51*, 1733−1746.
(30) Deo, G.; Turek, A. M.; Wachs, I. E.; Machej, T.; Haber, J.; Das, N.; Eckert, H.; Hirt, A. M. Physical and Chemical Characterization of Surface Vanadium Oxide Supported on Titania : Influence of the Titania Phase (Anatase , Rutile , Brookite and B). *Appl. Catal., A* **1992**, *91*, 27−42.
(31) Lu, S. W.; Harris, C.; Walck, S.; Arbab, M. Phase Sensitivity of Raman Spectroscopy Analysis of CVD Titania Thin Films. *J. Mater. Sci.* **2009**, *44*, 541−544.
(32) Balachandran, U.; Eror, N. G. Raman Spectra of Titanium Dioxide. *J. Solid State Chem.* **1982**, *42*, 276−282.
(33) Viswanathan, B.; Raj, K. J. A. Effect of Surface Area, Pore Volume and Particle Size of P25 Titania on the Phase Transformation of Anatase to Rutile. *Indian J. Chem., Sect. A: Inorg., Bio-inorg., Phys., Theor. Anal. Chem.* **2009**, *48*, 1378−1382.
(34) Ross-Medgaarden, E. I.; Wachs, I. E. Structural Determination of Bulk and Surface Tungsten Oxides with UV-Vis Diffuse Reflectance Spectroscopy and Raman Spectroscopy. *J. Phys. Chem. C* **2007**, *111*, 15089−15099.
(35) Magg, N.; Immaraporn, B.; Giorgi, J. B.; Schroeder, T.; Baumer, M.; Dobler, J.; Wu, Z.; Kondratenko, E.; Cherian, M.; Baerns, M.; et al. Vibrational Spectra of Alumina- and Silica-Supported Vanadia Revisited: An Experimental and Theoretical Model Catalyst Study. *J. Catal.* **2004**, *226*, 88−100.
(36) Baron, M.; Abbott, H.; Bondarchuk, O.; Stacchiola, D.; Uhl, A.; Shaikhutdinov, S.; Freund, H.-J.; Popa, C.; Ganduglia-Pirovano, M. V.; Sauer, J. Resolving the Atomic Structure of Vanadia Monolayer Catalysts : Monomers, Trimers, and Oligomers on Ceria. *Angew. Chem., Int. Ed.* **2009**, *48*, 8006−8009.
(37) Carrero, C. A.; Keturakis, C. J.; Orrego, A.; Schomäcker, R.; Wachs, I. E. Anomalous Reactivity of Supported V2O5 Nanoparticles for Propane Oxidative Dehydrogenation: Influence of the Vanadium Oxide Precursor. *Dalton Trans.* **2013**, *42*, 12644−12653.
(38) Hu, J. Z.; Xu, S.; Li, W.-Z.; Hu, M. Y.; Deng, X.; Dixon, D. A.; Vasiliu, M.; Craciun, R.; Wang, Y.; Bao, X.; et al. Investigation of the Structure and Active Sites of TiO2 Nanorod Supported VO. *ACS Catal.* **2015**, *5*, 3945−3952.
(39) Zhu, M.; Lai, J.-K.; Tumuluri, U.; Wu, Z.; Wachs, I. E. Nature of Active Sites and Surface Intermediates during SCR of NO with NH3 by Supported V2O5 −WO3/TiO2 Catalysts. *J. Am. Chem. Soc.* **2017**, *139*, 15624−15627.
(40) Hu, S.; Herner, J. D.; Shafer, M.; Robertson, W.; Schauer, J. J.; Dwyer, H.; Collins, J.; Huai, T.; Ayala, A. Metals Emitted from Heavy-Duty Diesel Vehicles Equipped with Advanced PM and NOX Emission Controls. *Atmos. Environ.* **2009**, *43*, 2950−2959.
(41) Liu, Z. G.; Ottinger, N. A.; Cremeens, C. M. Methods for Quantifying the Release of Vanadium from Engine Exhaust Aftertreatment Catalysts. *SAE Int. J. Engines* **2012**, *5*, 663−671.
(42) Liu, Z. G.; Ottinger, N. A.; Cremeens, C. M. Vanadium and Tungsten Release from V-Based Selective Catalytic Reduction Diesel Aftertreatment. *Atmos. Environ.* **2015**, *104*, 154−161.
(43) Hoej, J.; Beier, M. J. Vanadium-Based SCR Systems: Release of Vanadium and Tungsten during Operation and Possibilities for Reducing Vanadium Emissions. *SAE Int. J. Engines* **2014**, *7*, 1397−1400.
(44) Zhang, S.; Zhong, Q.; Zhao, W.; Li, Y. Surface Characterization Studies on F-Doped V2O5/TiO2 Catalyst for NO Reduction with NH3 at Low-Temperature. *Chem. Eng. J.* **2014**, *253*, 207−216.
(45) Kompio, P. G. W. A.; Brückner, A.; Hipler, F.; Auer, G.; Löffler, E.; Grünert, W. A New View on the Relations between Tungsten and Vanadium in V2O5WO3/TiO2 Catalysts for the Selective Reduction of NO with Nh3. *J. Catal.* **2012**, *286*, 237−247.
(46) Wachs, I. E.; Chan, S. S.; Chersich, C. C.; Saleh, R. Y. The Interaction of V2O5 with TiO2(Anatase): The Active Site for the Oxidation of O-Xylene to Phthalic Anhydride. *Stud. Surf. Sci. Catal.* **1984**, *19*, 275−282.
(47) Cole, D. J.; Cullis, C.; Hucknall, D. J. Studies of Heterogeneous Oxidation Catalysts-Part1. *J. Chem. Soc., Faraday Trans. 1* **1975**, *72*, 2185−2196.
(48) Cole, D. J.; Cullis, C. F.; Hucknall, D. J. Studies of Heterogeneous Oxidation Catalysts-Part2. *J. Chem. Soc., Faraday Trans. 1* **1976**, *72*, 2744−2752.
(49) Shubin, A. A.; Lapina, O. B.; Bosch, E.; Spengler, J.; Knozinger, H. Effect of Milling of V2O5 on the Local Environment of Vanadium as Studied by Solid-State 51V NMR and Complementary Methods. *J. Phys. Chem. B* **1999**, *103*, 3138−3144.
(50) Lapina, O. B.; Shubin, A. A.; Nosov, A. V.; Bosch, E.; Spengler, J.; Knözinger, H. Characterization of V2O5 - TiO2 Catalysts Prepared by Milling by ESR and Solid State 1H and 51V NMR. *J. Phys. Chem. B* **1999**, *103*, 7599−7606.
(51) Rasmussen, S. B.; Portela, R.; Bazin, P.; Ávila, P.; Bañares, M. A.; Daturi, M. Transient Operando Study on the NH3/NH4+ Interplay in V-SCR Monolithic Catalysts. *Appl. Catal., B* **2018**, *224*, 109−115.
(52) He, Y.; Ford, M. E.; Zhu, M.; Liu, Q.; Wu, Z.; Wachs, I. E. Selective Catalytic Reduction of NO by NH3 with WO3-TiO2

Catalysts: Influence of Catalyst Synthesis Method. *Appl. Catal., B* **2016**, *188*, 122−133.
(53) Wachs, I. E.; Deo, G.; Weckhuysen, B. M.; Andreini, A.; Vuurman, M. A.; Boer, M. d.; Amiridis, M. D. Selective Catalytic Reduction of NO with NH3 over Supported Vanadia Catalysts. *J. Catal.* **1996**, *161*, 211−221.
(54) Datka, J.; Turek, A. M.; Jehng, J.-M.; Wachs, I. E. Acidic Properties of Supported Niobium Oxide Catalysts : An Infrared Spectroscopy Investigation. *J. Catal.* **1992**, *135*, 186−199.
(55) Busca, G.; Lietti, L.; Ramis, G.; Berti, F. Chemical and Mechanistic Aspects of the Selective Catalytic Reduction of NOx by Ammonia over Oxide Catalysts : A Review. *Appl. Catal., B* **1998**, *18*, 1−36.
(56) Topsoe, N. Y.; Topsoe, H.; Dumesic, J. A. Vanadia/Titania Catalysts for Selective Catalytic Reduction (SCR) of Nitric Oxide by Ammonia. *J. Catal.* **1995**, *151*, 226−240.
(57) Topsoe, N. Y.; Dumesic, J. A.; Topsoe, H. Vanadia/Titania Catalysts for Selective Catalytic Reduction (SCR) of Nitric Oxide by Ammonia. *J. Catal.* **1995**, *151*, 241−252.

https://doi.org/10.1021/acscatal.1c02130
ACS Catal. 2021, 11, 12096−12111